1994-09

Vibration analysis of the AN/SPS-67(V)3 surface search radar

Tomaiko, Thomas A.

Monterey, California. Naval Postgraduate School

Approved for public release; distribution is unlimited.

Vibration Analysis of the AN/SPS-67(V)3
Surface Search Radar

by

Thomas A. Tomaiko
Lieutenant, United States Navy
B.S., United States Naval Academy, 1987

Submitted in partial fulfillment
of the requirements for the degree of

MASTER OF SCIENCE IN MECHANICAL ENGINEERING

from the

NAVAL POSTGRADUATE SCHOOL
September 1994

REPORT DOCUMENTATION PAGE

Form Approved OMB No. 0704

1. AGENCY USE ONLY	2. REPORT DATE	3. REPORT TYPE AND DATES COVERED
	September 1994	Master's Thesis

4. TITLE AND SUBTITLE: VIBRATION ANALYSIS OF THE AN/SPS-67(V)3 SURFACE SEARCH RADAR (U)

5. FUNDING NUMBERS

6. AUTHOR(S) Thomas A. Tomaiko

7. PERFORMING ORGANIZATION NAME(S) AND ADDRESS(ES)
Naval Postgraduate School
Monterey, CA 93943-5000

8. PERFORMING ORGANIZATION REPORT NUMBER

9. SPONSORING/MONITORING AGENCY NAME(S) AND ADDRESS(ES)

10. SPONSORING/MONITORING AGENCY REPORT NUMBER

11. SUPPLEMENTARY NOTES The views expressed in this thesis are those of the author and do not reflect the official policy or position of the Department of Defense or the U.S. Government.

12a. DISTRIBUTION/AVAILABILITY STATEMENT
Approved for public release; distribution is unlimited.

12b. DISTRIBUTION CODE
*A

13. ABSTRACT

Modern warships rely greatly upon electronic systems for their combat effectiveness, as well as defense. The ability of the U. S. Navy to maintain sea control and to project sea power depends upon the state-of-the-art combat systems equipment. Shipboard combat systems must, therefore, be shock hardened to be capable of operating in the combat shock environment.

The structural survivability of the mast and antennae and hence, the shipboard combat systems, is a shock induced vibration problem in which relatively low frequency equipment responses are observed. The structural survivability of combat systems can be "designed in" through the application of modern digital techniques for measuring and analyzing dynamic phenomena.

The purpose of this study was to build and demonstrate the practical value of a finite element model of the AN/SPS-67(V)3 surface search radar which when validated by experimentally obtained shock qualification data can serve as a powerful tool toward improving survivability of combat systems. The finite element model developed may be used to compute predicted shock-induced accelerations, velocities, displacements, and shock spectra resulting from UNDEX in order to evaluate the potential for antenna structural survivability or vulnerability on an existing platform. Furthermore, the antenna finite element model may be used in the design of new mast-antenna systems.

14. SUBJECT TERMS

AN/APS-67(V)3 Surface Radar, Finite Element Code, Modal Analysis, Dynamic Response

15. NUMBER OF PAGES 131

16. PRICE CODE

17. SECURITY CLASSIFICATION OF REPORT	18. SECURITY CLASSIFICATION OF THIS PAGE	19. SECURITY CLASSIFICATION OF ABSTRACT	20. LIMITATION OF ABSTRACT
Unclassified	Unclassified	Unclassified	UL

NSN 7540-01-280-5500

Standard Form 298 (Rev. 2-89)
Prescribed by ANSI STD. 239-18

ABSTRACT

Modern warships rely greatly upon electronic systems for their combat effectiveness, as well as defense. The ability of the U. S. Navy to maintain sea control and to project sea power depends upon the state-of-the-art combat systems equipment. Shipboard combat systems must, therefore, be shock hardened to be capable of operating in the combat shock environment.

The structural survivability of the mast and antennae and hence, the shipboard combat systems, is a shock induced vibration problem in which relatively low frequency equipment responses are observed. The structural survivability of combat systems can be "designed in" through the application of modern digital techniques for measuring and analyzing dynamic phenomena.

The purpose of this study was to build and demonstrate the practical value of a finite element model of the AN/SPS-67(V)3 surface search radar which when validated by experimentally obtained shock qualification data can serve as a powerful tool toward improving survivability of combat systems. The finite element model developed may be used to compute predicted shock-induced accelerations, velocities, displacements and shock spectra resulting from UNDEX in order to evaluate the potential for antenna structural survivability or vulnerability on an existing platform. Furthermore the antenna finite element model may be used in the design of new mast-antenna systems.

Table of Contents

ACKNOWLEDGEMENT

The author is grateful for the support of this work by the Naval Postgraduate School and the Naval Sea Systems Command, Washington DC. The completion of this research project was due to the support and guidance of many. The author would like to thank Dr. Y.S. Shin and Dr. J.H. Gordis for their guidance. A special thanks to Mr. Mark McLean and Mr. Victor DiRienzo of the Naval Sea Systems Command and Mr. Charles Connors and Mr. Nick Parella of Norden Systems, Inc., Melville NY, for their efforts. In addition, the author is especially grateful for the support and encouragement of his father, Mr. Andrew J. Tomaiko, Jr. Finally, the author wishes to give special thanks to Ms. Denise M. Fragolletti who inspired the author with her patience and understanding.

I. INTRODUCTION

A. DESCRIPTION OF THE AN/SPS-67(V)3 SURFACE SEARCH RADAR SYSTEM

The AN/SPS-67(V)3 surface search radar designed by Norden Systems, Inc., a subsidiary of United Technologies, is the current state-of-the-art replacement for the most widely used radar in the U.S. Navy, the AN/SPS-10 surface search radar. It is especially notable for being the first Navy radar constructed with standard electronic modules (SEMs) which give it improved reliability, maintainability, and performance. Currently, over 125 AN/SPS-67(V) surface search radar systems have been delivered to the U.S. and foreign navies [Ref. 1]. The AN/SPS-67 surface search radar family includes- AN/SPS-67(V)1, AN/SPS-67(V)2, and AN/SPS-67(V)3 versions.

The AN/SPS-67(V) is a 2-D surface surveillance radar that operates at C-band. Initially, with the introduction of the AN/SPS-67(V)1, C-band was selected because it permitted the use of the existing AN/SPS-10 antenna system. Only the below deck equipment was replaced with new solid state cabinets. The AN/SPS-67(V)1 features enhanced video clutter suppression, sharper video performance and anti-jamming capability. The AN/SPS-67(V)2 features a new antenna, shown in Figure 1.1, which increases the vertical beam-width from

17 to 31.5 degrees. This enables the AN/SPS—67(V)2 to detect additional targets. The new antenna also features a built—in IFF antenna and two scan rates (15 and 30 rpm).

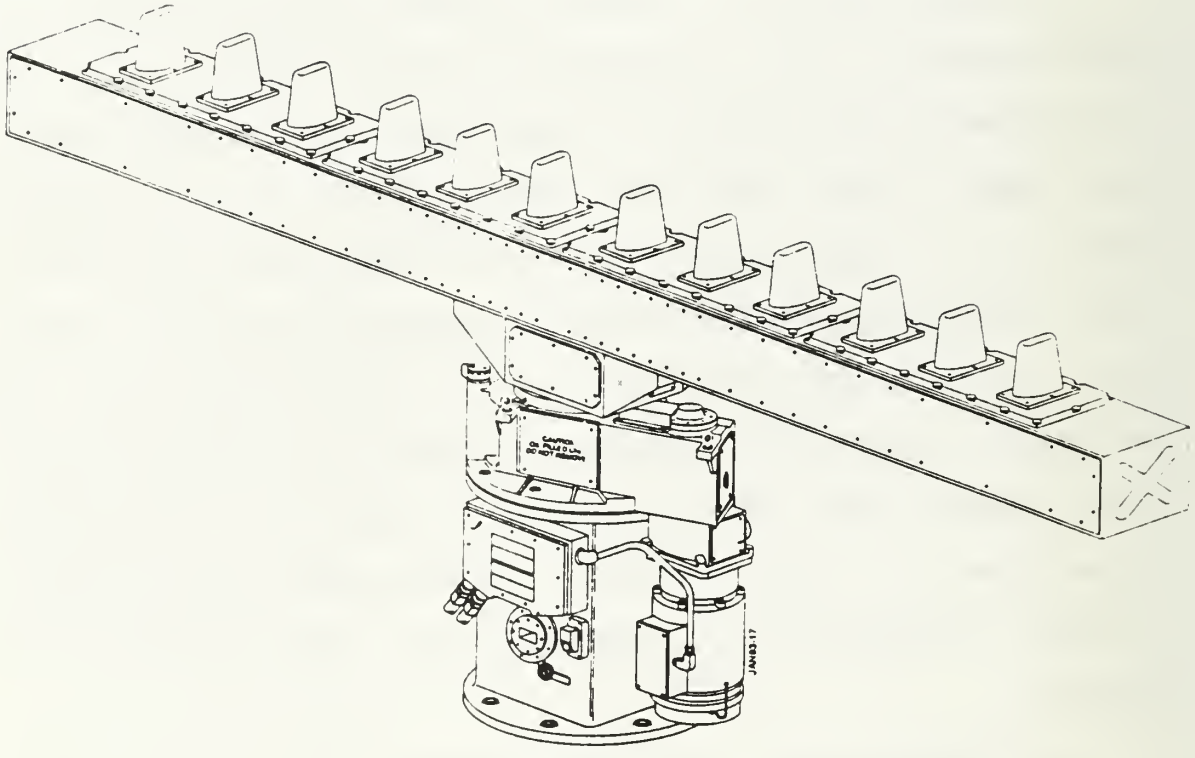

FIGURE 1.1: THE AN/SPS—67(V) 2&3 SURFACE SEARCH RADAR ANTENNA ASSEMBLY. COURTESY NORDEN SYSTEMS, INC.

The latest version, AN/SPS—67(V)3 surface search radar, features a new signal processor. Its improved frequency stability and the addition of a digital moving target indicator (DMTI) and automatic target detector (ATD) provide

improved surveillance and detection of low-flying and surface targets and permits operation of the AN/SPS-67(V)3 with integrated automatic detection and tracking (IADT) systems. The AN/SPS-67(V)3 has a gunfire control interface which provides accurate data for gun fire support and reduces the target detection components of combat systems' radar reaction time. Norden Systems, Inc. is presently delivering the AN/SPS-67(V)3 version for the U.S. Navy, USS ARLEIGH BURKE (DDG-51) class of ships.

B. PROBLEM DEFINITION

Modern warships rely greatly upon electronic systems for their combat effectiveness, as well as defense. The ability of the U.S. Navy to maintain sea control and to project sea power depends upon the state-of-the-art combat systems equipment. Shipboard combat systems must, therefore, be shock hardened to be capable of operating in the combat shock environment. The underwater explosion (UNDEX) of conventional or nuclear weapons in proximity of a naval ship will induce severe excitation of shipboard combat systems, which may produce failures, thereby limiting or eliminating the combat effectiveness of the ship.

A major component of every radar system is its antenna. Most radar antennae are located on the ship's main mast. The main mast provides for the maximum height possible of shipboard radar antennae for maximum range of detection of

targets. A ship's mast and antennae system must be designed to withstand moderate to severe shock loading induced by underwater explosion (UNDEX). The UNDEX produces a large and rapid evolution of energy resulting in enormous destructive power delivered to the ship in the form of incident shock wave pressure, gas bubble oscillation, cavitation closure pulses, and various reflection wave effects. These shock-induced forces propagate through the ship and top-side structures, including the mast and antennae.

The response of the mast and antennae to UNDEX is basically vibrational in nature subjected to base excitation. The mast and antennae tend to vibrate at their fundamental natural frequency or at a low range of natural frequencies typically between 0-33 hertz, since the ship acts as a low pass mechanical filter, passing relatively low frequency components of the propagating shock wave. The peak amplitude usually occurs well after the shock wave passes the ship.

The structural survivability of the mast and antennae and hence, the shipboard combat systems, is thus a vibration problem in which relatively low frequency equipment support excitations are observed. The ability of a U.S. Naval warship to carryout its mission after being subjected to an UNDEX depends on the survivability of its shipboard combat systems. Thus, in addition to meeting the operational requirements of the weapons system, the electronic equipment, specifically the radar antennae, must be designed to withstand the adverse

effects of UNDEX. The structural survivability of combat systems subjected to weapons effects can be "designed in" through the application of modern digital techniques for measuring and analyzing dynamic phenomena. Recently, a modal survey of the USS JOHN PAUL JONES (DDG-53) main mast structure and mast-mounted antennae was conducted. The modal test results successively confirmed the vibrational characteristics of the total structure previously predicted by structural dynamic analysis [Ref. 2].

The purpose of this study was to build and demonstrate the practical value of a finite element model of the AN/SPS-67 (V) 3 surface search radar which when validated by experimentally obtained shock qualification data can serve as a powerful design tool toward improving survivability of combat systems. The modal analysis was performed to characterize the vibration behavior of the AN/SPS—67 (V) 3 antenna assembly. The frequency response analysis was also performed in order to better understand the antenna dynamics. The finite element model developed may be used to predict shock-induced accelerations, velocities, displacements and shock spectra resulting from UNDEX in order to evaluate the potential for antenna structural survivability or vulnerability on an existing platform. Furthermore, the antenna finite element model may be used in the design of new mast/antenna systems. The advantage of such an approach is the ability to design mast/antenna systems with the optimal

placement of antennae for shock hardening. The effectiveness of such an approach far exceeds all other methods currently employed in mast/antennae shock hardening.

C. SCOPE OF RESEARCH

This study documents the development of the finite element representation of the AN/SPS-67(V)3 surface search radar antenna and pedestal. The finite element model was developed using an advanced finite element code called I-DEAS (Integrated Design Engineering Analysis) which is developed and supported by the Structural Dynamics Research Corporation (SDRC). The finite element model was used to solve for the normal modes of oscillation. In addition, frequency response analysis yielded frequency response functions for the finite element model which was compared to response shock spectra obtained from the antenna's shock qualification test. The finite element model was then corrected and validated.

The development of the model, design decisions, and supporting theory are the scope of this thesis.

In Chapter II, the basic theoretical and practical background of normal mode dynamics are discussed. The development of the AN/SPS-67(V)3 finite element model are discussed in Chapter III. In Chapter IV, the normal modes of vibration for the AN/SPS-67(V)3 surface search radar and the frequency response analysis of the AN/SPS-67(V)3 surface search radar are discussed. Suggestions for future work and

shock testing of shipboard systems are discussed in Chapter V. Conclusions are listed in Chapter VI.

D. MOTIVATION

Motivation for this research project was provided by Mr. Mark McLean's Mechanical Engineering Seminar, Modal Test of USS JOHN PAUL JONES (DDG—53) Mast and Mast—mounted Antennas, held at the Naval Postgraduate School on 14 January 1993, and the NAVSEA sponsored research program titled Shipboard Systems Survivability: Dynamic Design Analysis and Testing Methods and Live Fire Test Simulation.

The development of modern digital techniques for measuring and analyzing dynamic phenomena has led to a new method for determining the structural survivability of shipboard combat systems subjected to weapons effects. This methodology uses modal test data obtained from a shipboard modal test survey and the analytic model obtained from finite element analysis. The finite element model, when validated and corrected by the true modal parameters identified from the modal test, provides substantially improved predictions of the modal parameters. The corrected finite element model may then be used in subsequent analytical studies to evaluate and optimize proposed combat system designs for survivability and simulation of actual live fire test and evaluation (LFT&E).

For new combat system designs, a modal test is not possible and, therefore, a finite element model of the system is required. However, if a finite element model is to serve as an accurate predictive tool, the modal parameters, as calculated from the finite element analysis, must be validated against the measured modal parameters. The initial program of research proposes to model and test a variety of existing masts and antennae. Such a program will generate a structural dynamics database of existing designs which can be used to extrapolate to new designs. Furthermore, the modeling and testing of existing masts and antennae will generate the modeling and analysis methods and criteria required to ensure that finite element models of new designs will yield accurate estimates of the modal parameters, even if a modal test is not possible.

II. BACKGROUND

A. FINITE ELEMENT MODELING

The finite element method (FEM) is a numerical procedure for solving the problems encountered in engineering which cannot be solved analytically. It is especially useful for solving problems which involve irregular-shaped structures made up of a variety of materials and physical discontinuities such as changes in thickness, holes, etc. Finite element methods yield an approximate solution of the theoretical behavior of a structure at a finite set of points specified in the model called nodes. These nodes occur at the interconnection of a finite number of elements which subdivide the structure. The process of finite element modeling consists of building a suitable idealization of the structure made of these nodes and elements. The accuracy of the model solution depends largely on the idealization of the structure, the number of nodes and elements and type of elements used. Thus, finite element modeling is an engineering approximation which is limited in accuracy, but may be used to yield valuable information about a structure's behavior. The finite element engineer must ensure the proper element type and density are chosen to accurately represent the structure.

Although the concept of finite element modeling has been around since the 1950s, the method has only recently become feasible with the aide of computers. The finite element method applies several mathematical concepts to solve a system of governing equations over the domain of the structure. The number of equations is usually very large, depending upon the number of physical degrees of freedom (DOF), and requires the computational power of today's computers. The art of finite element modeling is to discretize, or divide, the structure into finite elements without using an excessively large number of elements. As the number of finite elements increases, the accuracy of the solution increases, however, this also increases the computation time and storage required for the solution. The finite element engineer must use sound engineering judgment when developing a model in order to balance the cost and benefit associated with increasing the number of discretizations.

B. NORMAL MODE ANALYSIS

Normal mode analysis is a method for predicting the undamped natural frequencies and corresponding mode shapes of vibration for structures. Mode shapes and natural frequencies are used to predict transient load points and frequencies which can generate significant structural responses. If the excitation frequency is close to a natural frequency, it may

produce an undesirably large response. Furthermore, mode shapes can identify what load locations and directions will excite the structure.

The equation of motion can be written as follows:

$$[M]\{\ddot{q}\} + [K]\{q\} = \{0\} \tag{2.1}$$

where $[M]$ represents the structure mass matrix, $\{\ddot{q}\}$ is the node acceleration vector, $[K]$ is the structure stiffness matrix, and $\{q\}$ is the node displacement vector.

Equation (2.1) represents a system of fully-coupled equations involving n independent unknowns. The unknowns are the physical coordinates $\{q\}$. The solution to Equation (2.1) may be obtained by assuming a solution of the form:

$$\{q\} = C\{\phi\} e^{j\omega t} \tag{2.2}$$

where C is a complex constant, $\{\phi\}$ is a spatial vector and $e^{j\omega t}$ is a time-dependent scalar. Substituting Equation (2.2) and its derivatives into Equation (2.1) yields an nth-order homogeneous algebraic eigenvalue problem of the form:

$$\left[-\omega^2[M] + [K]\right] C\{\phi\} e^{j\omega t} = \{0\} \tag{2.3}$$

The non-trivial solution to Equation (2.3) requires:

$$\det[[K] - \omega^2[M]] = \{0\} \tag{2.4}$$

Equation (2.4) is the characteristic equation whose roots are the eigenvalues, $\lambda = \omega^2$. Corresponding to each eigenvalue, ω^2, is an eigenvector, $\{\phi\}$. Therefore, the solution to the free vibration problem is n eigenpairs, ω_n and $\{\phi^n\}$. Each eigenvector, $\{\phi^i\}$, is orthogonal to every other eigenvector. This property of orthogonality permits any mode of vibration to be represented by a linear combination of these eigenvectors, or mode shapes. Using Equation (2.3), the nodal displacements may be written as:

$$\begin{Bmatrix} q_1(t) \\ q_2(t) \\ q_3(t) \\ \vdots \\ q_n(t) \end{Bmatrix} = \begin{Bmatrix} \phi_1^1 \\ \phi_2^1 \\ \phi_3^1 \\ \vdots \\ \phi_n^1 \end{Bmatrix} C_1 e^{j\omega_1 t} + \begin{Bmatrix} \phi_1^2 \\ \phi_2^2 \\ \phi_3^2 \\ \vdots \\ \phi_n^2 \end{Bmatrix} C_2 e^{j\omega_2 t} + \begin{Bmatrix} \phi_1^3 \\ \phi_2^3 \\ \phi_3^3 \\ \vdots \\ \phi_n^3 \end{Bmatrix} C_3 e^{j\omega_3 t} + \ldots + \begin{Bmatrix} \phi_1^n \\ \phi_2^n \\ \phi_3^n \\ \vdots \\ \phi_n^n \end{Bmatrix} C_n e^{j\omega_n t} \tag{2.5}$$

and

$$\begin{Bmatrix} q_1(t) \\ q_2(t) \\ q_3(t) \\ \vdots \\ q_n(t) \end{Bmatrix} = \left[\{\phi^1\} \{\phi^2\} \{\phi^3\} \ldots \{\phi^n\} \right] \begin{Bmatrix} u_1(t) \\ u_2(t) \\ u_3(t) \\ \vdots \\ u_n(t) \end{Bmatrix}$$

where

$$[\Phi] = \left[\{\phi^1\} \{\phi^2\} \{\phi^3\} \ldots \{\phi^n\} \right]$$

The q(t)'s are the physical coordinates of the nodal displacements and $[\Phi]$ is a transformation matrix which transforms the physical coordinates to modal coordinates, $\{u(t)\}$.

Invoking the property of orthogonality, Equation (2.5) states that at any instant of time, t, when the system has a configuration $\{q(t)\}$, this configuration can be exactly represented by appropriately combining n constant homogeneous vectors, $\{\phi^i\}$. The coefficients of combination are functions of time known as modal coordinates.

For systems involving many degrees of freedom (DOF), the n coupled equations of motion are difficult to solve. Therefore, a method which diagonalizes the [K] and [M] matrices is used. Once the diagonalized [K] and [M] matrices are obtained, the equations of motion become fully uncoupled and the solution then becomes one of solving n independent homogeneous differential equations. The method which diagonalizes the [K] and [M] matrices, thereby decoupling the equations of motion, is called modal decomposition. The method is facilitated by the linear transformation from physical coordinates to modal coordinates via the transformation (modal) matrix $[\Phi]$. Premultipying by the

transpose of the modal matrix diagonalizes the mass and stiffness matrices. The result is:

$$[M]\{\ddot{u}(t)\} + [K]\{u(t)\} = \{0\} \tag{2.6}$$

The ith row of the above diagonalized equations of motion may be written as:

$$M_{ii}\,\ddot{u}_i + K_{ii}\,u_i = 0 \tag{2.7}$$

Multiplying Equation (2.7) through by $\frac{1}{M_{ii}}$ yields:

$$\ddot{u}_i + \omega_i^2\,u_i = 0 \tag{2.8}$$

where

$$\omega_i^2 = \frac{K_{ii}}{M_{ii}}$$

III. MODEL DEVELOPMENT

The purpose of this Chapter is to discuss the development of the AN/SPS-67(V)3 surface search radar antenna finite element model and to document the design decisions which were made based on the antenna's fabrication drawings and technical manuals.

The finite element model (FEM) was built and analyzed using I-DEAS Simulation which is a mechanical computer-aided engineering tool that allows the user to build a complete finite element model, including physical and material properties, loads, and boundary conditions. First, a solid model of the antenna and pedestal was created using I-DEAS Modeling. The solid model was developed using the antenna's fabrication drawings and represents the antenna and pedestal's structural components including its physical and material properties. The purpose of the solid model was to completely describe the antenna and pedestal as closely as possible.

The finite element model was then created by manually creating nodes and elements using the solid model as a reference. Features of the solid model, such as bolt-holes, fillets, and covers, that do not appreciably effect the dynamic analysis, were removed. Also, dimensions were reduced

during the transformation of the solid model by choosing appropriate elements to represent each structural component. The finite element model was completed by defining physical and material properties for each element. Once completed, the finite element model was solved for the normal modes of oscillation using the Simultaneous Vector Iteration (SVI) Method. The FEM process used is summarized in Figure 3.1.

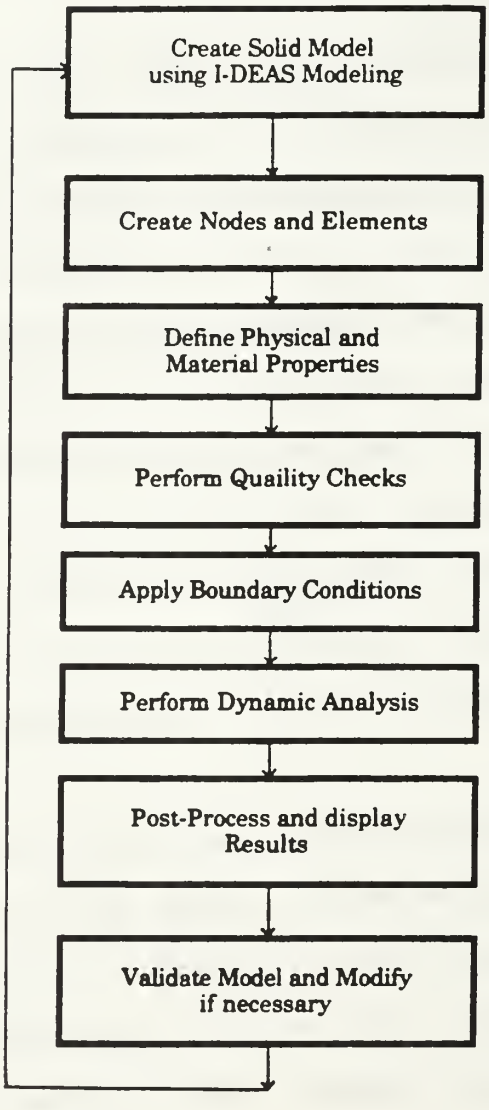

FIGURE 3.1: THE FEM PROCESS

A. SOLID MODELING

The first step in the finite element modeling process was to create a geometric or solid model of the antenna assembly. This section provides a brief overview of the antenna assembly, the assembly parts and the construction of the solid model representation.

1. Description of the AN/SPS-67(V)3 Antenna Assembly

The AN/SPS-67(V)3 antenna assembly consists of two major structural components, the antenna sub-assembly and the pedestal assembly. The antenna sub-assembly, shown in Figure 3.2, consists of both a C-band antenna for use with the AN/SPS-67 radar and an IFF antenna for use with existing shipboard IFF equipment. The C-band antenna is an end-fed traveling wave array that uses inclined slots cut into the narrow wall of the waveguide to couple electromagnetic (EM) power into the 64 horn radiators. The waveguide and the horns are enclosed in the antenna housing. The housing has a flat front cover, C-band radome, and a convex rear cover. The IFF antenna consists of 12 pairs of radiating elements which are enclosed by 12 IFF radomes and are mounted on top of the C-band antenna housing by 4 IFF divider networks. The antenna is connected to the pedestal by use of an adapter box and a spindle.

The pedestal assembly, shown in Figure 3.3, rotates the antenna sub-assembly at either 15 or 30 rpm. The pedestal assembly includes a two-speed motor running at 1800 or 3600

rpm, and a motor transmission which reduces the motor rpm to the desired antenna rotation rate. The motor housing is attached to the gear housing and is positioned vertically along side the pedestal. The transmission gears which rotate the antenna sub-assembly are enclosed in the gear housing. In addition, the pedestal assembly includes a two speed syncro data unit which transmits the bearing angle position of the antenna to the below decks antenna controller for processing into antenna bearing data.

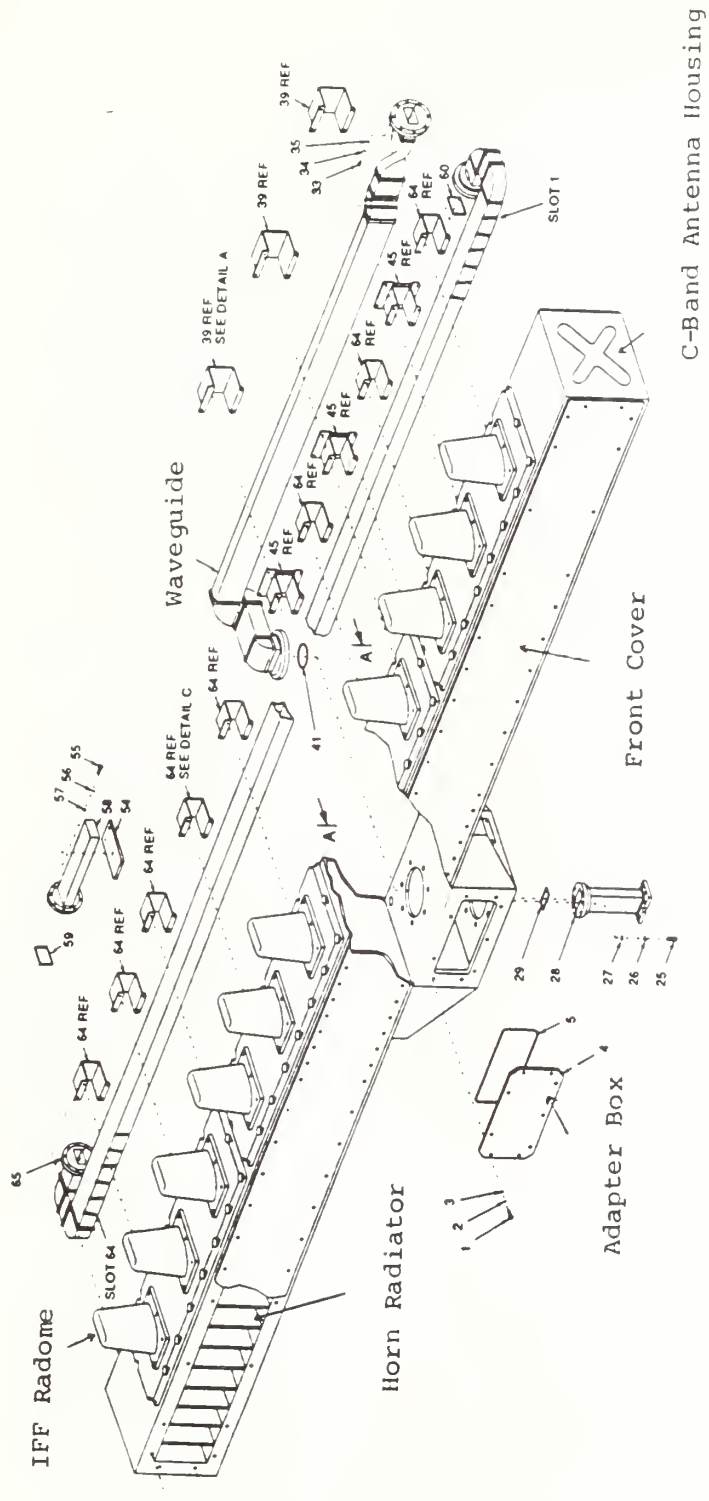

FIGURE 3.2: AN/SPS-67(V)3 ANTENNA SUB-ASSEMBLY DRAWING. COURTESY NORDEN SYSTEMS, INC.

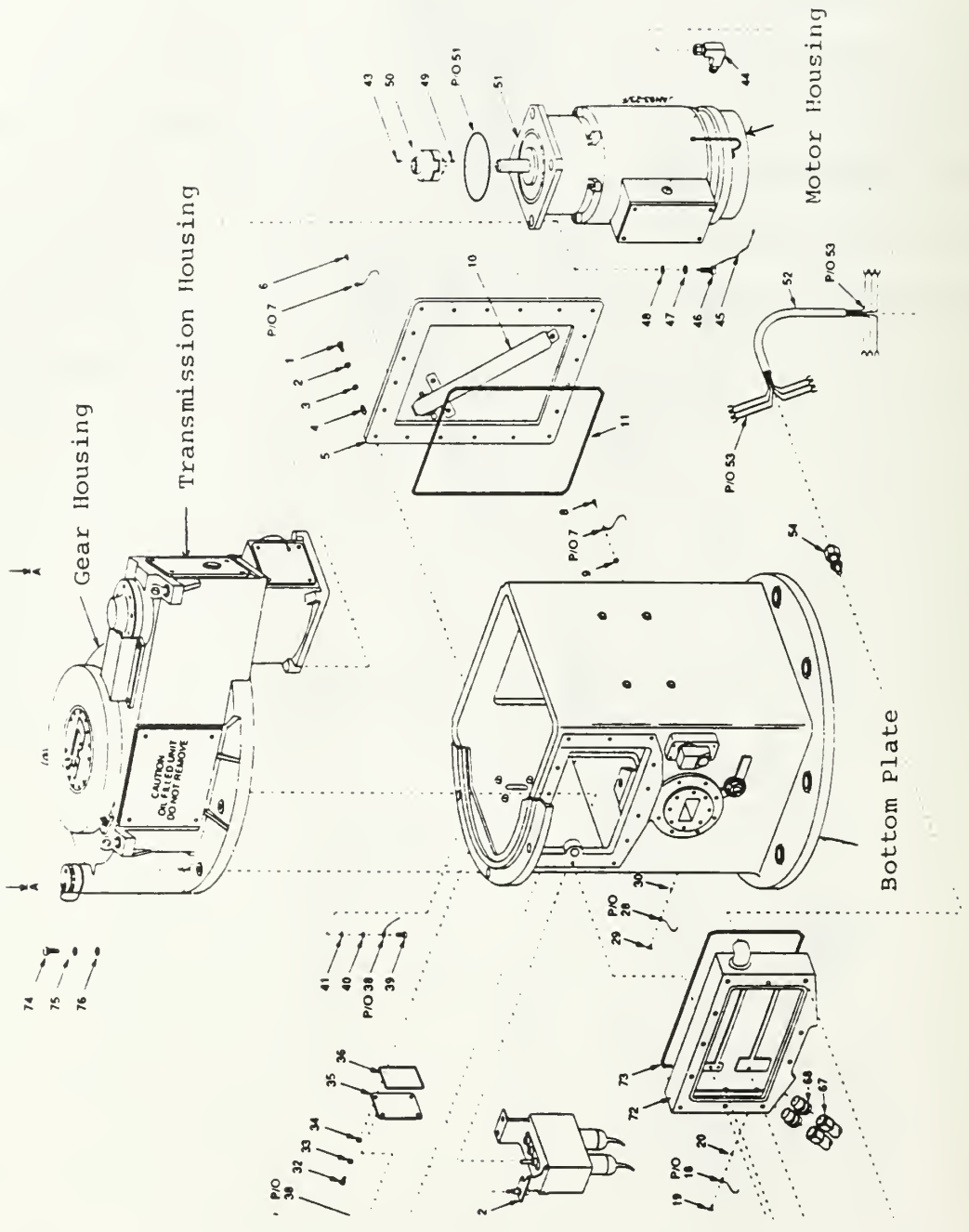

FIGURE 3.3: AN/SPS—67(V)3 PEDESTAL ASSEMBLY DRAWING. COURTESY NORDEN SYSTEMS, INC.

2. Part Creation

The I—DEAS Modeling task provides the modeling tools needed to develop detailed parts. Parts are generally created by extruding or revolving 2D profiles and orienting, cutting, or joining objects. The dimensions and constraints are user defined and can be modified. Parts are created on the workbench, the workbench is the work area used to create, modify, and select parts, and are stored in bins. Table 3.1 lists the parts created with I—DEAS Master Modeler and the fabrication drawing(s) used to obtain the correct physical and material properties.

TABLE 3.1: SOLID MODEL PARTS

PART	Fabrication Drawing No.
Antenna	167702
Antenna Rear Cover	177508
Radome C Band (Front Cover)	177587
IFF Divider Network	177540, 177545, 177548
IFF Radome	177588
Adapter Box	177515
Spindle	177265
Shroud	177268
Gear Housing	177262
Gear Housing Side Cover	177262
Pedestal Plate, Top	177295
Pedestal Midsection	177295
Access Cover	177302
Data Unit Cover	177309
Junction Box Cover	177321, 177329
Motor Housing	177208
Pedestal Bottom	177295

3. Construction Operations

Once the major structural components were modeled with an associated part, the parts were modified by construction operations which include cutting, joining, and intersecting with different objects in order to construct the completely assembled antenna. For the Simulation Application, the Master Modeler by itself was enough to model the assembled antenna geometry. Figure 3.4 shows a shaded image of the completely assembled antenna.

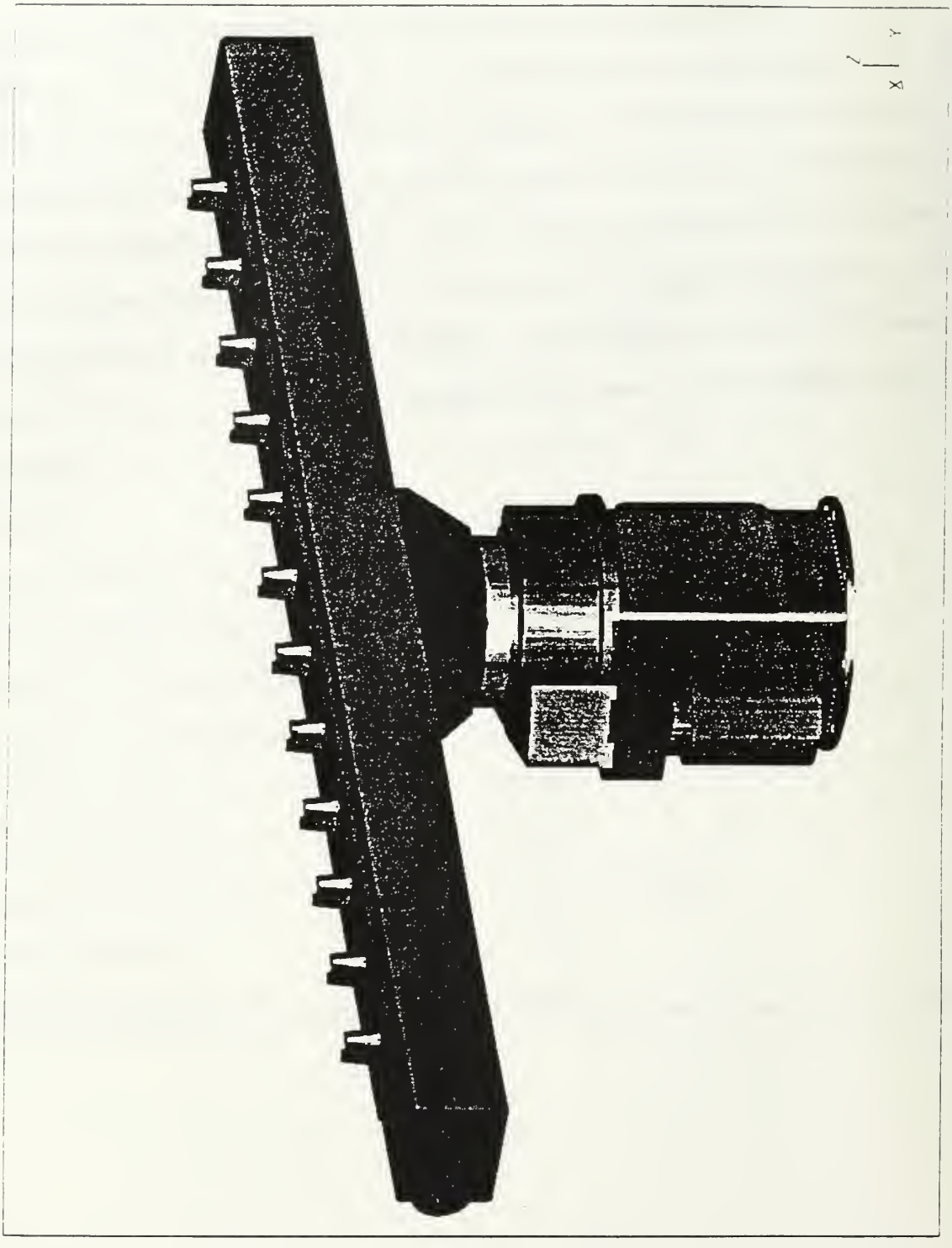

FIGURE 3.4: SHADED—IMAGE OF THE AN/SPS—67(V)3 SOLID MODEL.

B. MESH GENERATION

The solid model representation of the antenna assembly was built with as much attention to detail as possible. Once created, the solid model served as a template which can be accessed in the Meshing Task. The next step in the finite element process was to generate nodes and elements on the existing geometry developed in the Master Modeler Task. At this point, it was apparent that the geometry from the solid model was too refined, and that some idealizations of the geometry were necessary in order to generate a suitable mesh. The design decisions made are too numerous to mention specifically, however, the primary methods used were feature suppression and dimension reduction.

1. Node Creation

Each node is a coordinate point in 3D space. A node can have up to six degrees of freedom (DOF) depending on the element type. The finite element formulation will have one equation for each DOF at all the nodes at the boundary of an element. The unknowns are the nodal displacements. Nodes were created manually by keying in their coordinates or generated by copying, reflecting, or generating nodes between two sets of nodes. The finite element model contains 2984 nodes.

2. **Element Creation**

There are several different types of elements. No one element is best for all cases, therefore, each element was selected for the particular structure it represented. The accuracy of the finite element solution depends on the modeler's correct judgment when selecting the type of element. The element chosen must be sufficient to model the structure's response to in-service loads. Each element was created manually by picking nodes defining the element, i.e., four nodes for a quadrilateral shell element. The finite element model contains 3577 elements.

The antenna finite element (FE) model contains several types of elements including – beam elements, shell elements, spring elements, and rigid elements.

Beam elements are one-dimensional elements which require two nodes, one at each end-point. Beam elements are defined in I-DEAS Beam Section by using standard sections or by creating them manually. These elements can be used to represent structures where length is much greater than its transverse dimension. Beam elements were used to model the spindle. Since the spindle has varying cross-section, several elements, with varying cross-section dimensions, were used.

Shell elements are two-dimensional elements whose thickness is small compared to its length and width. Shell elements require nodes at each corner. These elements can be used to represent structures that are thin with respect to

its other dimensions. Thin shell elements were used to represent most of the structural components of the antenna assembly including – the pedestal casing, the gear housing, and the antenna sub–assembly.

Spring elements were used in the FE model to represent the duplexed, radial contact ball bearings. Both translational and rotational spring elements were used. The node–to–node translational spring element models linear elastic springs and is defined between two nodes. The node–to–node rotational spring element models torsional springs and is defined between two nodes. The spring stiffness, which represents the force required to separate the nodes a unit displacement, is specified with respect to the global coordinate system axes.

Rigid elements are massless, infinitely stiff elements used to restrict the motion of the nodes of an element so that they move together. Rigid elements were used in the FE model to represent the shaft connections between the adapter box and the antenna pedestal and also to facilitate the placement of lumped mass elements in the model.

3. Finite Element Model Components

Figure 3.5 is an assembly drawing which shows the completely assembled antenna. The antenna sub–assembly is coupled with the antenna pedestal by the shaft connection. The shaft connection consists of the spindle and bearing

assembly. The following discussion focuses on the major FE model components.

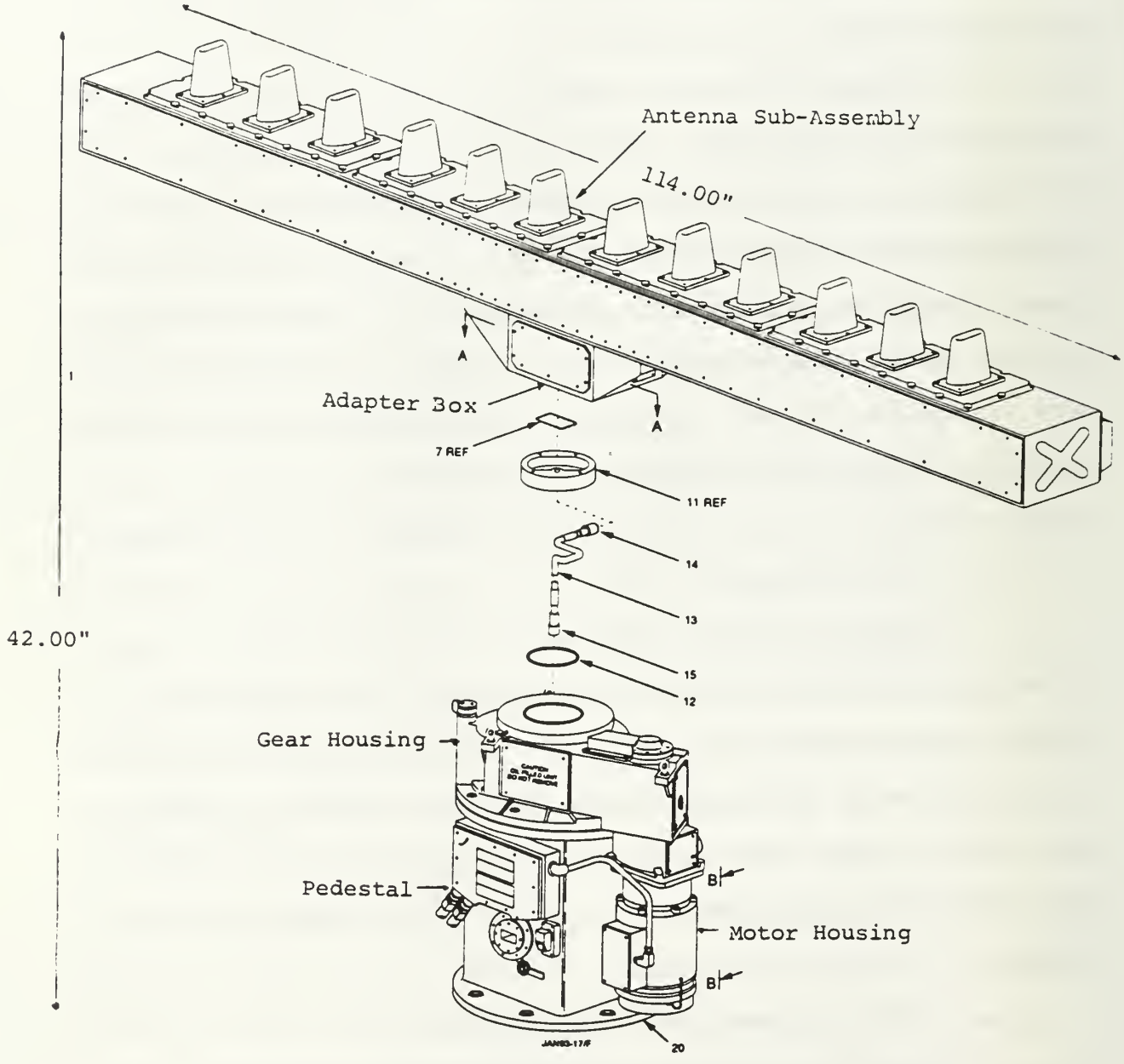

FIGURE 3.5: AN/SPS—67(V)3 ASSEMBLY DRAWING. COURTESY NORDEN SYSTEMS, INC.

a. Antenna Sub—assembly

The antenna sub—assembly was created using thin shell elements. Lumped masses were used to model additional nonstructural mass not represented by the shell elements, i.e., the IFF radome elements and waveguide. The antenna sub—assembly is analogous to a beam restrained at its mid—span, and it has physical properties which make it less stiff relative to the pedestal. Therefore, the antenna sub—assembly was expected to be the primary structural component involved in the solution of the normal modes of vibration. As evidenced by the results, the antenna sub—assembly is, in fact, the primary structural component in the solution of the normal modes.

Two different finite element (FE) models of the antenna sub—assembly were created. The first involved the use of 3400 shell elements and is shown in Figure 3.6. The second version used 2318 shell elements and is shown in Figure 3.7. Both FE models were restrained by enforcing zero displacement at each of the four corners of the adapter box. The two FE models were solved and the solutions were compared. The mode shapes were identical and their corresponding frequencies did not change significantly. Therefore, the FE model with fewer elements was chosen in order to reduce the number of degrees of freedom while maintaining a sufficient number of elements to accurately model the antenna sub—assembly. Table 3.2 lists the natural

frequencies for the first 10 modes of vibration for both FE models. The mode shape plots are included in Appendix A.

TABLE 3.2: ANTENNA SUB-ASSEMBLY FE MODEL COMPARSION.

MODE	NATURAL FREQUENCY (HZ)	
	2318 SHELL ELEMENTS	3400 SHELL ELEMENTS
1	58.22	57.39
2	62.18	59.71
3	93.08	91.68
4	106.96	100.44
5	267.06	208.99
6	290.33	290.00
7	383.28	382.74
8	409.10	398.10
9	436.88	432.57
10	442.30	435.93

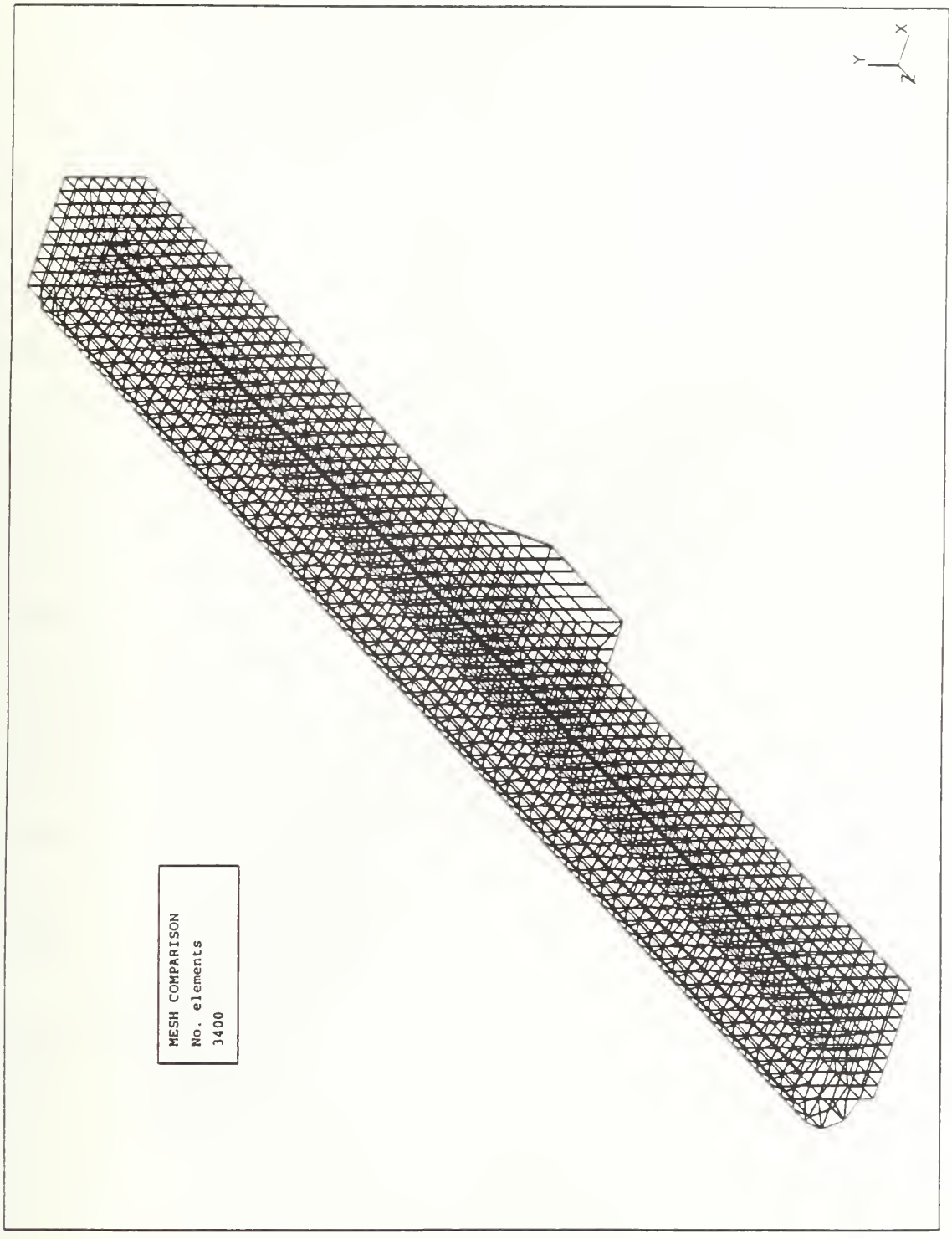

FIGURE 3.6: ANTENNA SUB—ASSEMBLY (3400 ELEMENTS).

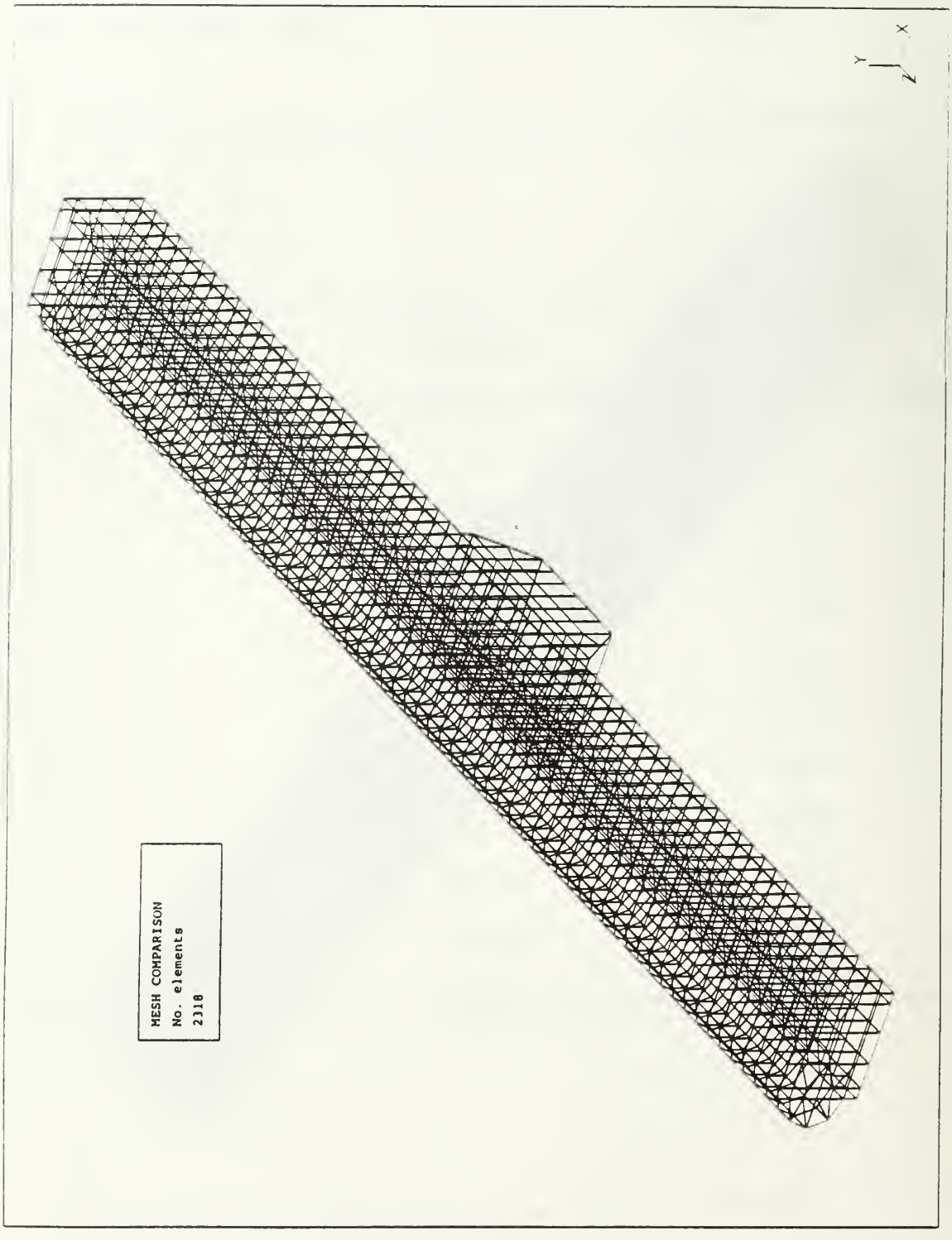

FIGURE 3.7: AN ANNA SUB-ASSEMBLY (2318 ELEMENTS).

b. Shaft Connection

The shaft connection, shown in Figure 3.8, consists of the FE model elements used to represent the spindle and bearing assembly. It couples the antenna sub-assembly and the pedestal while allowing the antenna sub-assembly to rotate. The spindle was modeled using beam elements. The two beam cross sections used are shown in Figures 3.9 and 3.10. The connections between the spindle and the adapter box and the bearing assembly were modeled with rigid elements. The duplexed, radial contact ball bearings were modeled using node-to-node translational and node-to-node rotational springs. The bearings were modeled in great detail, since they are a primary load path in the FE model between the antenna sub-assembly and the pedestal. The bearings provide axial, as well as, radial support of the spindle. The bearing stiffness values were supplied by the bearing manufacturer for a free race analysis and does not account for the shaft and housing. The free race radial, axial, and moment stiffnesses are summarized in Table 3.3.

The manufacture's free race analyses are included in Appendix B.

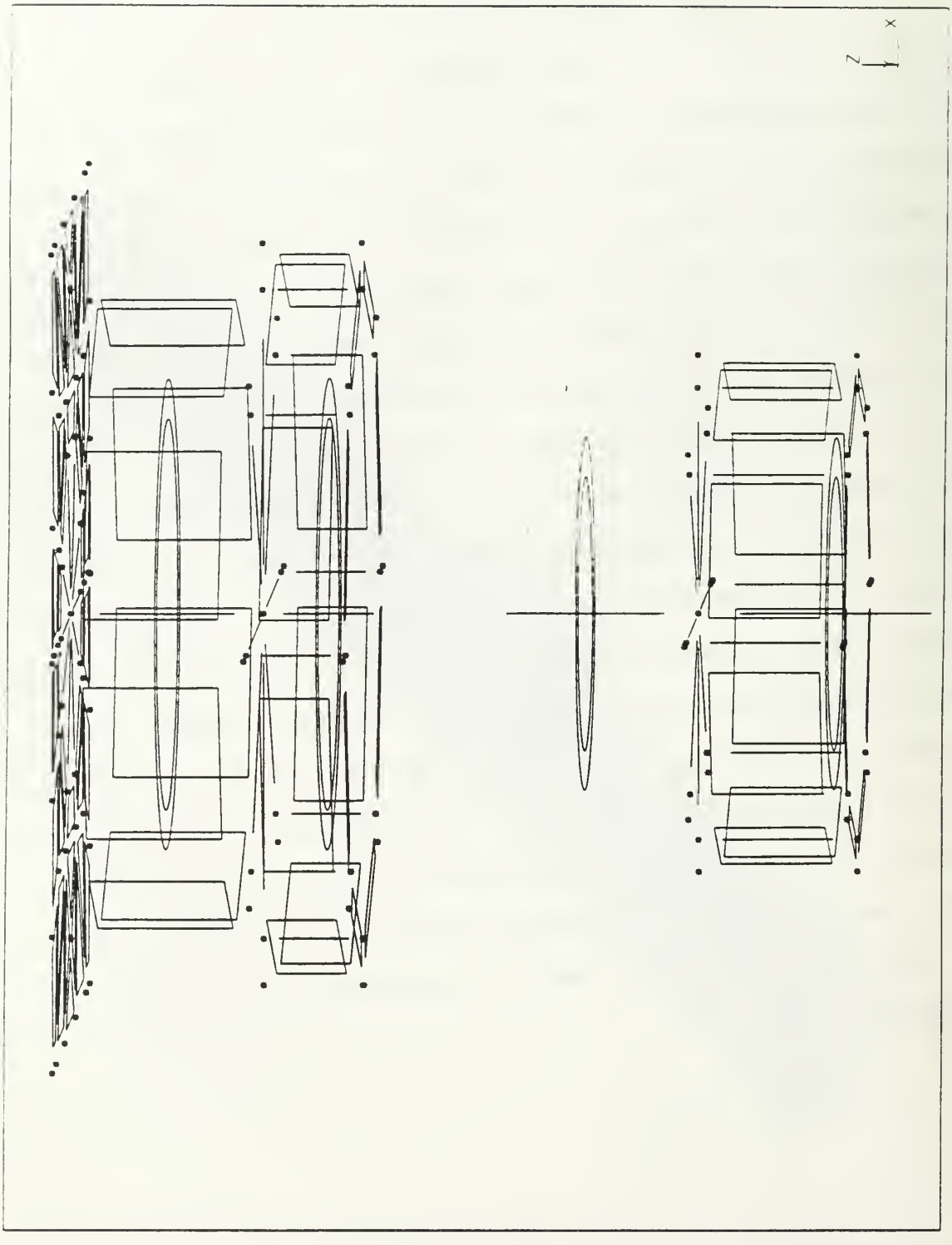

FIGURE 3.8: SHAFT CONNECTION.

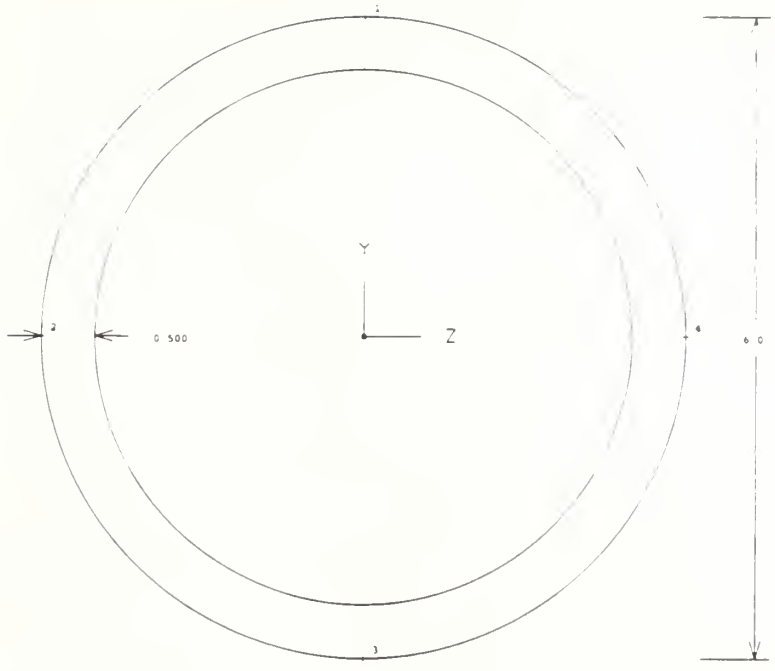

FIGURE 3.9: BEAM CROSS-SECTION (6.0 IN).

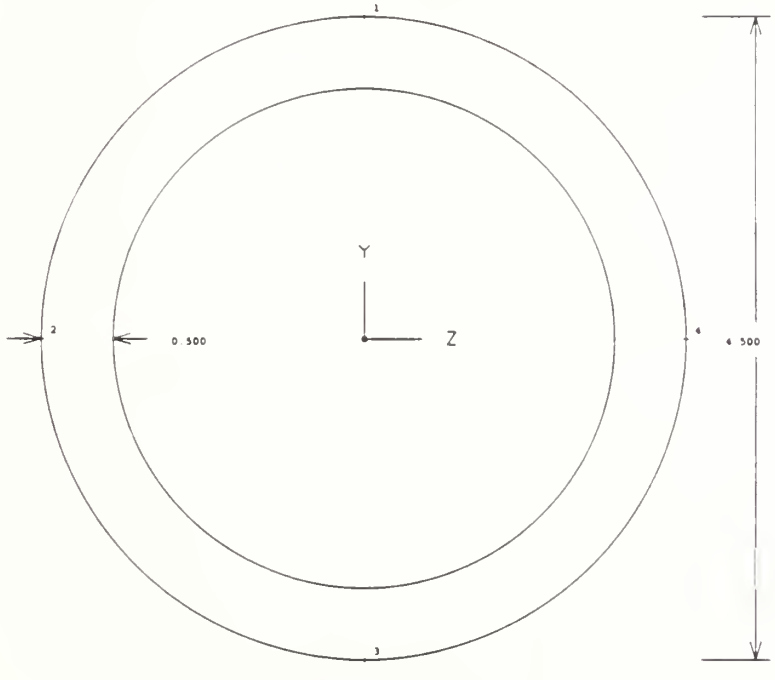

FIGURE 3.10: BEAM CROSS-SECTION (4.5 IN).

TABLE 3.3: FREE RACE RADIAL, AXIAL, AND MOMENT STIFFNESSES

	STIFFNESSES (X 10^6 LB/IN)		
BEARING	RADIAL	AXIAL	MOMENT
8IN X 6IN	2.59	1.32	20.1
6IN X 4.5IN	0.718	0.0400	0.477

There are 8 elements spaced symmetrically around the circumference of the bearing. They connect the spindle to the pedestal gear housing. The bearing stiffnesses ($K_{bearing}$) were resolved using Hooke's Law in order to calculate the effective spring stiffnesses (K_{eff}) for each of the 8 elements. Hooke's Law states:

$$F = K_{TOTAL}\, X \tag{3.1}$$

From Figure 3.11, the forces acting on the bearing may be summed as follows:

$$F_1 = \frac{K_{TOTAL}}{\cos 0^\circ} X, \tag{3.2}$$

and

$$F_2 = \frac{K_{TOTAL}}{\cos 45^\circ} X, \text{ etc.} \tag{3.3}$$

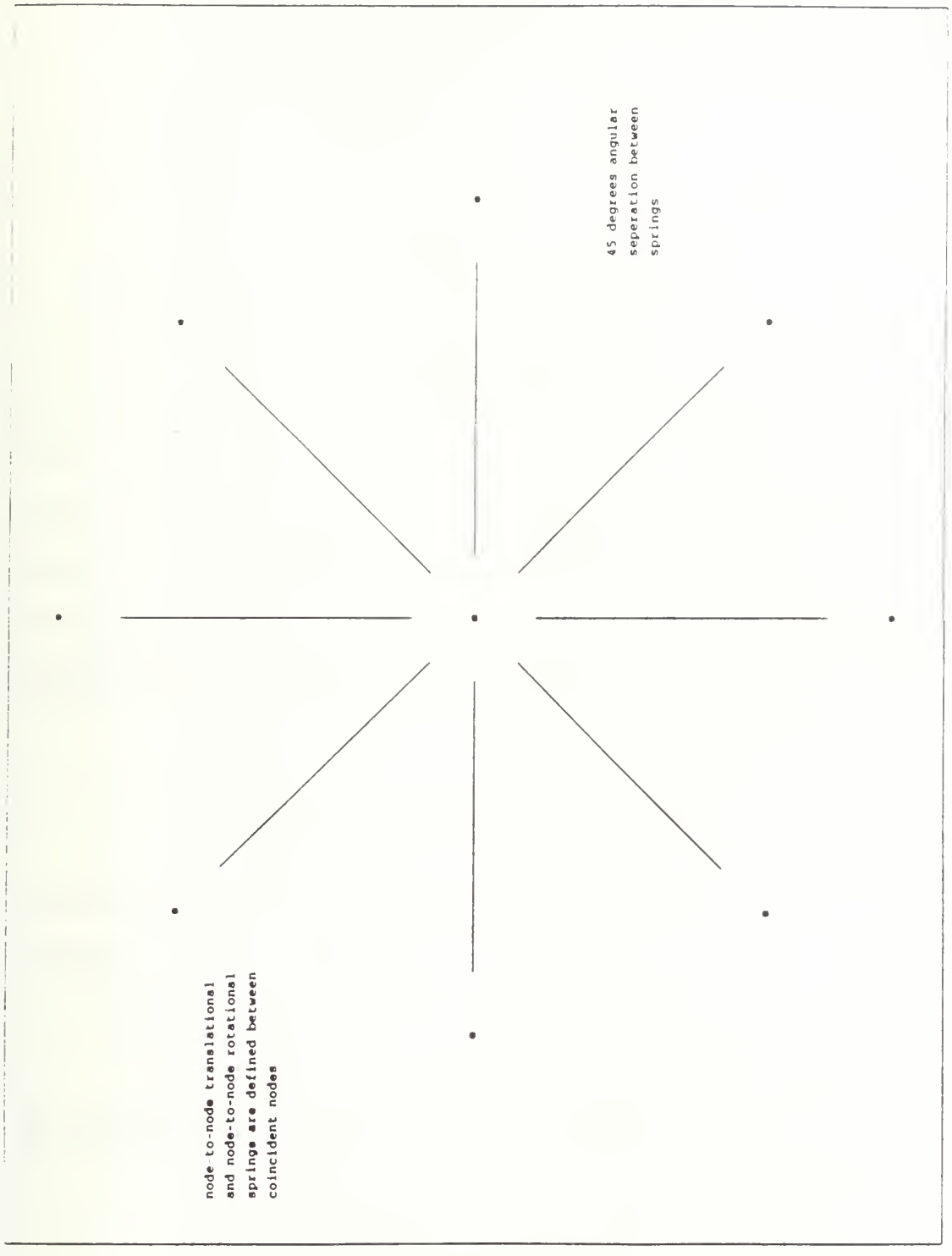

FIGURE 3.11: DUPLEXED, RADIAL CONTACT BALL BEARING GEOMETRY.

Solving Equation (3.1) for K_{TOTAL} and setting $K_{TOTAL} = K_{bearing}$ yields:

$$K_{bearing} = \sum_{i=0}^{8} K_{eff} \cos \alpha_i \qquad (3.4)$$

where

$$K_{eff} = \frac{K_{bearing}}{f}$$

and

$$f = \cos 0° + \cos 45° + \cos 90° + \ldots + \cos 315°$$

The resulting effective spring stiffnesses are summarized in Table 3.4.

TABLE 3.4: EFFECTIVE SPRING STIFFNESSES (K_{eff})

	STIFFNESSES (X 10^6 LB/IN)		
BEARING	**RADIAL**	**AXIAL**	**MOMENT**
8IN X 6IN	**0.536**	**0.273**	**4.16**
6IN X 4.5IN	**0.149**	**0.00828**	**0.0988**

c. Pedestal Assembly

The pedestal assembly was created using thin shell elements. Lumped masses were used to model additional mass not represented by the shell elements, i.e., the motor and transmission gears.

C. DEFINING PHYSICAL AND MATERIAL PROPERTIES

Every element in the finite element (FE) model has been assigned physical and material properties consistent with the solid model representation of the antenna. Physical properties are the geometric properties of an element. They represent, for example, shell element thickness, beam cross-section and spring stiffness. Table 3.5 lists the physical property table referenced by the elements in the FE model.

TABLE 3.5 PHYSICAL PROPERTY TABLE

PHYSICAL PROPERTY NAME	SHELL THICKNESS (IN)	SPRING STIFFNESS ($X10^5$ LB/IN)	MASS (LB)
Antenna Top Middle	0.625		
Antenna Top Sides	0.125		
Antenna Front Cover	0.5		
Antenna Front T&B	0.125		
Antenna Bottom	0.125		
Antenna Rear Cover	0.09		
Antenna Rear T&B	0.375		
Antenna Sides	0.125		
Antenna Horn Fins	0.062		
Antenna Horn Center	0.125		
Adapter Top	0.315		
Adapter Sides	0.19		
Adapter Bottom	0.87		
Gear Housing Top	0.25		
Gear Housing Sides	0.25		
Gear Housing Side	0.85		

PHYSICAL PROPERTY NAME	SHELL THICKNESS (IN)	SPRING STIFFNESS ($X10^5$ LB/IN)	MASS (LB)
Pedestal Top Plate	1.12		
Pedestal Side	0.50		
Pedestal Sides	0.78		
Pedestal Sides	0.34		
Pedestal Bottom Plate	0.57		
Junction Box	0.38		
Junction Box cover	0.19		
Access Cover	0.19		
Data Unit Cover	0.19		
Motor Trans Gear Box	0.38		
Motor Trans Gear Box Bottom	0.76		
Motor Case	1.0		
Motor Case	0.81		
Motor Case	0.38		
Bearing Retainer	1.0		
Bearing	0.25		
Cartridge Upper Bearing	0.25		
Cartridge Lower Ball Bearing XX (8IN x 6IN)		5.37 0.0 2.73	

PHYSICAL PROPERTY NAME	SHELL THICKNESS (IN)	SPRING STIFFNESS ($X10^5$ LB/IN)	MASS (LB)
Ball Bearing XY		3.79	
(8IN X 6IN)		3.79	
		2.73	
Ball Bearing YY		0.0	
(8IN X 6IN)		5.37	
		2.73	
Ball Bearing		1.49	
XX (6INX4.5IN)		0.0	
		0.0828	
Ball Bearing XY		1.05	
(6INX4.5IN)		1.05	
		0.0828	
Ball Bearing YY		0.0	
(6INX4.5IN)		1.49	
		0.0828	
Ball Bearing		0.0	
Rotational XX		41.6	
(8IN X 6IN)		0.0	
Ball Bearing		29.4	
Rotational XY		29.4	
(8IN X 6IN)		0.0	
Ball Bearing		41.6	
Rotational YY		0.0	
(8IN X 6IN)		0.0	
Ball Bearing		0.0	
Rotational XX		0.988	
(6IN X 4.5IN)		0.0	
Ball Bearing		0.699	
Rotational XY		0.699	
6IN X 4.5IN)		0.0	

PHYSICAL PROPERTY NAME	SHELL THICKNESS (IN)	SPRING STIFFNESS ($X10^5$ LB/IN)	MASS (LB)
Ball Bearing		0.988	
Rotational YY		0.0	
(6IN X 4.5IN)		0.0	
IFF Radome			2.0
Wave Guide			2.0
Spindle Gears			70.0
Motor			50.0
Motor Gear Box			30.0
Gear House Gears			30.0

Each element has material properties. The material property table contains the Young's Modulus (E), Poison's Ratio(ν), and mass density (γ) for every element in the FE model. Table 3.6 lists the material property table referenced by the elements.

TABLE 3.6: MATERIAL PROPERTY TABLE

Material Property Name	Young's Modulus (E) ($X10^6$ psi)	Poison's Ratio (ν)	Mass Density (ρ) ($X10^{-4}\frac{lbf\text{-}s^2}{in^4}$)
A356.0T6	10.5	0.34	2.5124
A357.0T6	10.4	0.34	2.5124
6061–T651	10.0	0.33	2.5265
E GLASS	10.5	0.34	2.3829
5052	10.2	0.33	2.5124
304SS	28.0	0.29	7.5139

D. PERFORMING MESH QUALITY CHECKS

I–DEAS Meshing Task can check the finite element model for modeling errors such as duplicate nodes and elements, missing elements, and check element warping and distortion. The free element edge check will plot the free edges of elements not connected to another element [Ref. 3]. Normally, this will plot the boundaries of the model. However, if elements adjoin each other edge to edge, but reference duplicate coincident nodes rather than share the same nodes, a crack will appear in the FE model. A missing line indicates duplicate elements sharing the same nodes [Ref. 4]. Node coincident check will check nodes that are very close together. Coincident nodes may be merged, if desired [Ref.5].

Element distortion is used to highlight elements that are distorted. Distorted check lists elements with values ranging from 0.0 to 1.0. A value of 1.0 represents a perfect square [Ref. 6]. Ideally thin shells would have a distortion value of 1.0, however, values between 0.5 and 1.0 are acceptable.

E. BOUNDARY CONDITIONS

Prior to solving the finite element (FE) model for the normal modes, the FE model boundary conditions must be specified. The antenna boundary conditions are in the form of restraints. Restraints are used to enforce displacement on specified nodes or geometry. The antenna model has eight bolt holes located on the pedestal bottom plate that mount the antenna to the main mast, thereby preventing rigid body motion of the FE model. The antenna has one restraint set which consists of zero displacement enforced at each of the eight bolt hole locations.

The completed finite element (FE) model of the AN/SPS-67 (V)3 antenna assembly is shown in Figures 3.12 and 3.13.

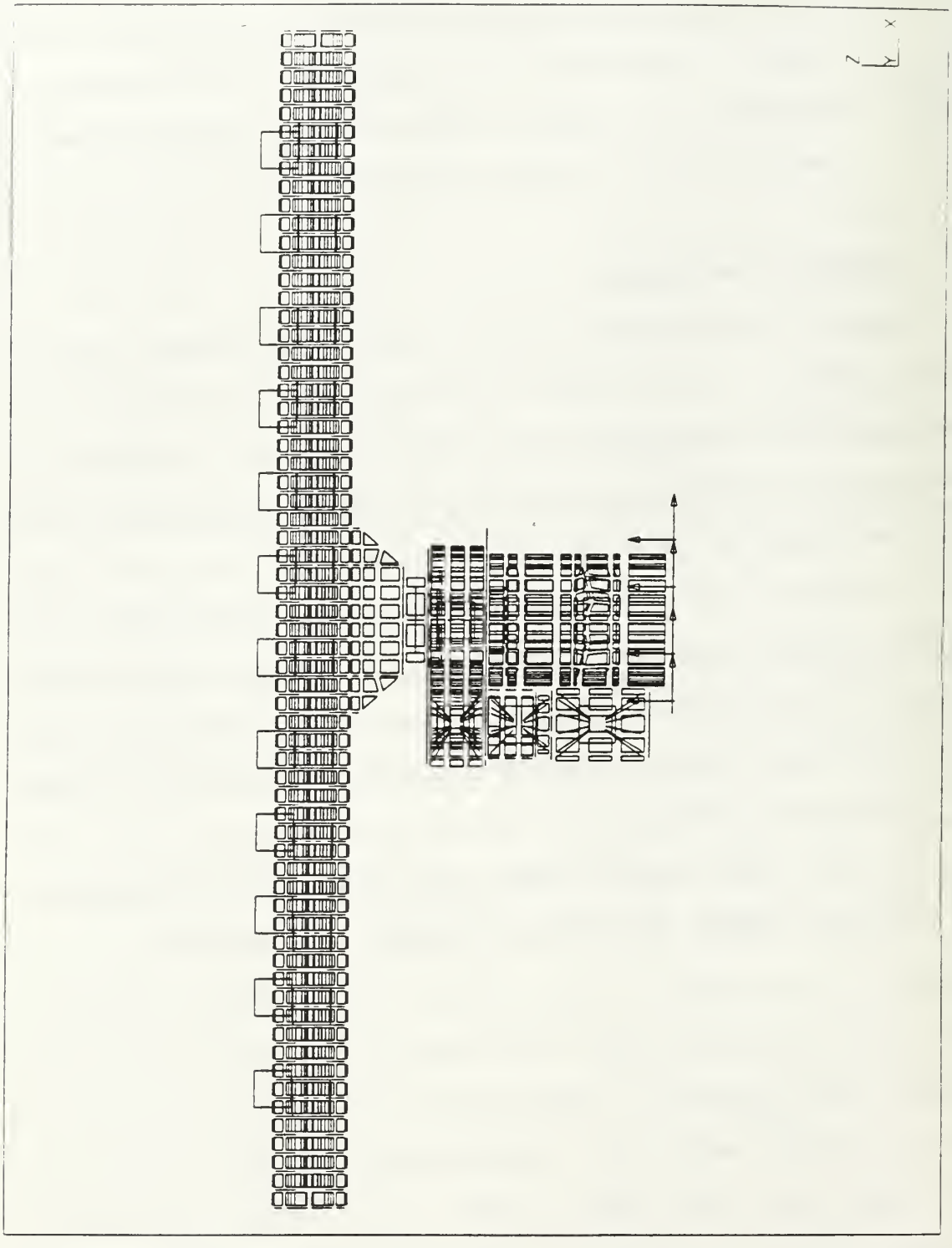

FIGURE 3.12: COMPLETED ANTENNA FE MODEL.

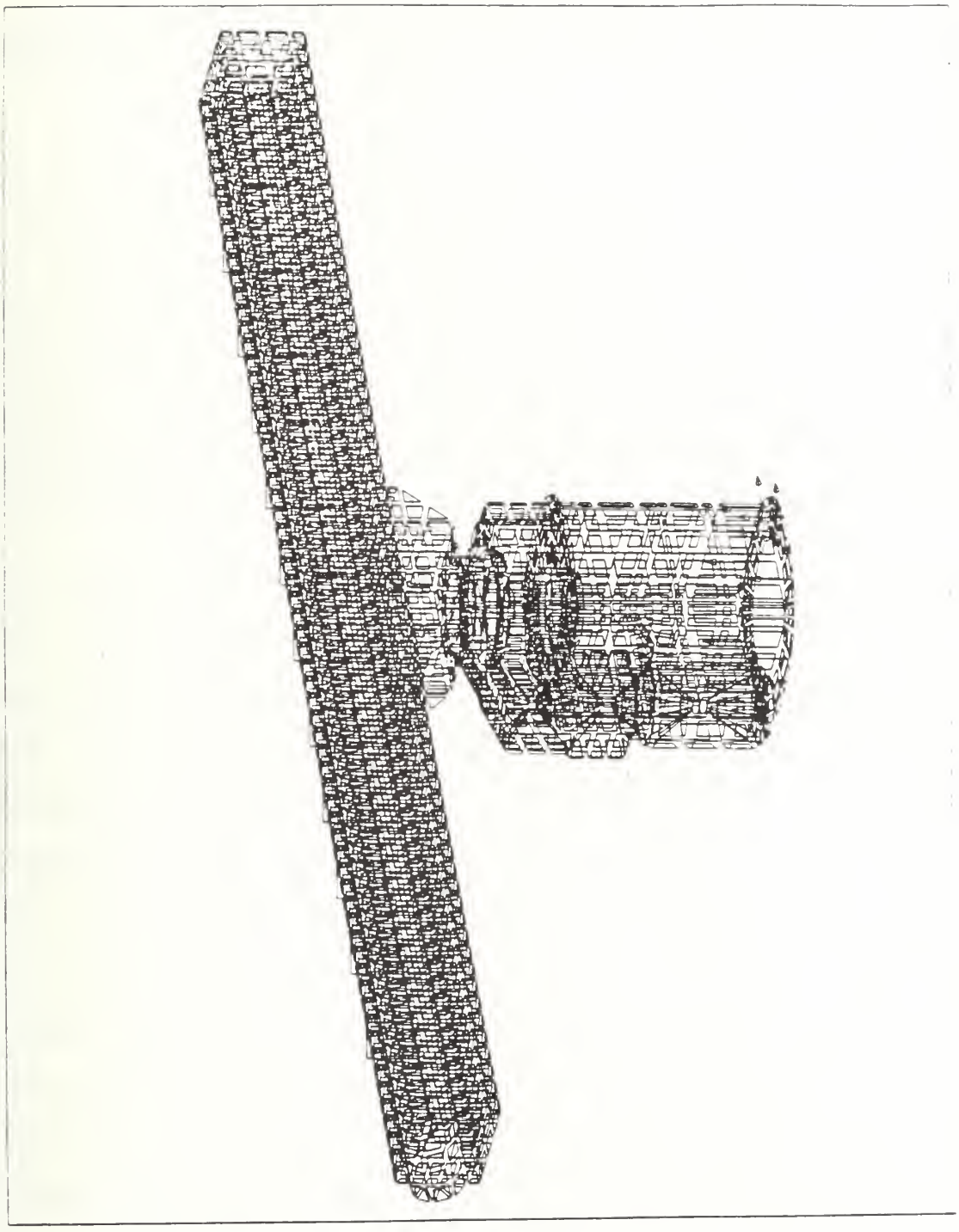

FIGURE 3.13: ISOMETRIC VIEW OF COMPLETED ANTENNA

IV. NORMAL MODES AND TRANSIENT RESPONSE

A. MODEL SOLUTION

The antenna finite element model normal mode dynamics were solved using the Model Solution Task. Solving for the normal modes involves calculating the natural frequencies and mode shapes of the antenna. I—DEAS provides three methods for solving the normal mode, eigenvalue problem — Guyan Reduction, Simultaneous Vector Iteration (SVI), and Lanczos. The SVI method was used.

The SVI method is one the most efficient method for solving models with many degrees of freedom (DOF). The solution begins with a set of starting vectors which are iteratively refined until convergence is reached. The accuracy of the convergence and the number of converged flexible modes are specified by the user. The SVI method performs the solution on full matrices. No master DOF selection is required. The SVI solution allows the user to select the solution output. The first twenty modes were solved in approximately four hours on a Hewlett Packard 735 Workstation. There are 17,904 DOF in the antenna finite element model. The natural frequencies of these modes range from 16 to 494 Hertz. Table 4.1 lists the modes and

frequencies. Figures 4.1 through 4.20 contain all 20 modes, in ascending order by frequency.

The first three modes occur near the low frequency range of interest, from 0 to 33 hz. All three modes represent antenna–pedestal interaction modes. The natural frequencies at which these modes occur depends largely on the design of the upper and lower duplexed, radial contact ball bearings and the shaft connections. Comparison of several different designs yielded the optimum design. The mode shapes seem reasonable and are as expected from the antenna sub–assembly normal mode solution.

TABLE 4.1: AN/SPS-67(V)3 ANTENNA MODES BY ASCENDING FREQUENCY

MODE	NATURAL FREQUENCY PREDICTED (HZ)	DESCRIPTION	NATURAL FREQUENCY TEST (HZ)
1	16.82	Antenna Sub-assembly rigid body (lateral) roll	14.8
2	27.22	Antenna Sub-assembly rigid body yaw	23.8
3	34.22	Antenna Sub-assembly rigid body (fore/aft) pitch	31.8
4	56.71	Antenna Pedestal lateral rocking and Antenna Sub-assembly (lateral) roll	
5	65.36	Antenna Sub-assembly rigid body heave and Antenna Sub-assembly first bending (in phase)	
6	100.97	Antenna Pedestal fore/aft rocking and Antenna Sub-assembly pitch	
7	127.60	Antenna Sub-assembly rigid body heave and Antenna Sub-assembly first bending (out of phase)	
8	152.18	Motor Pendulum	
9	154.82	Antenna Sub-assembly fore/aft first bending and Antenna Sub-assembly pitching	
10	202.43	Antenna Pedestal lateral rocking and Antenna Sub-assembly second bending	

MODE	FREQUENCY (HZ)	DESCRIPTION
11	229.66	Motor Pendulum
12	295.31	Antenna Pedestal heave and Antenna Sub-assembly second bending (vertical)
13	359.31	Antenna Sub-assembly torsion
14	370.56	Antenna Sub-assembly torsion
15	399.61	Antenna Sub-assembly fore/aft second bending
16	415.90	Antenna Sub-asssembly lateral second bending and torsion
17	444.44	Antenna Sub-assembly symmetric second bending (vertical)
18	462.47	Antenna Pedestal panel mode
19	484.51	Antenna Pedestal panel mode
20	494.03	Antenna pedestal panel mode

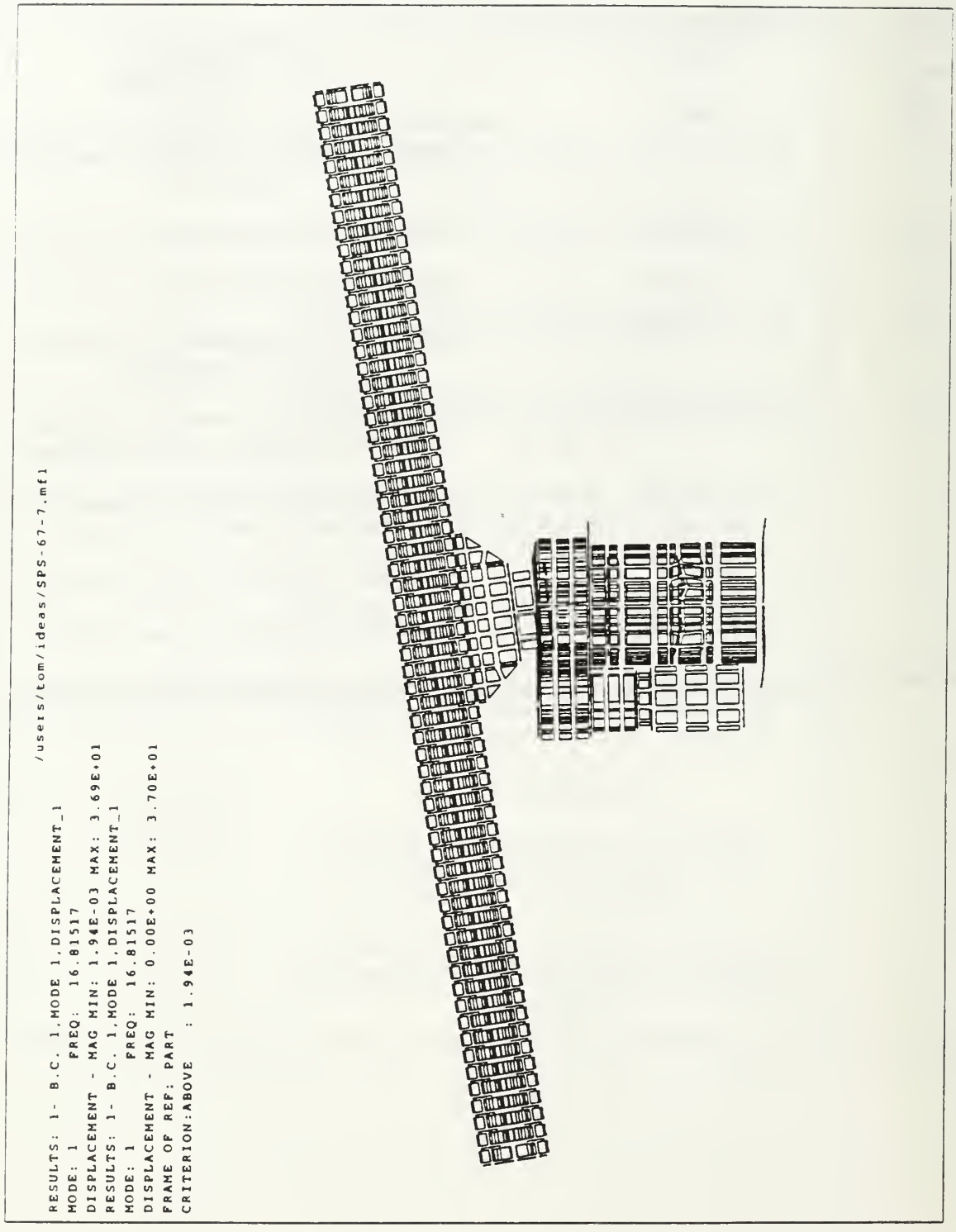

FIGURE 4.1: MODE 1 (FRONT VIEW)

FIGURE 4.2: MODE 2 (TOP VIEW)

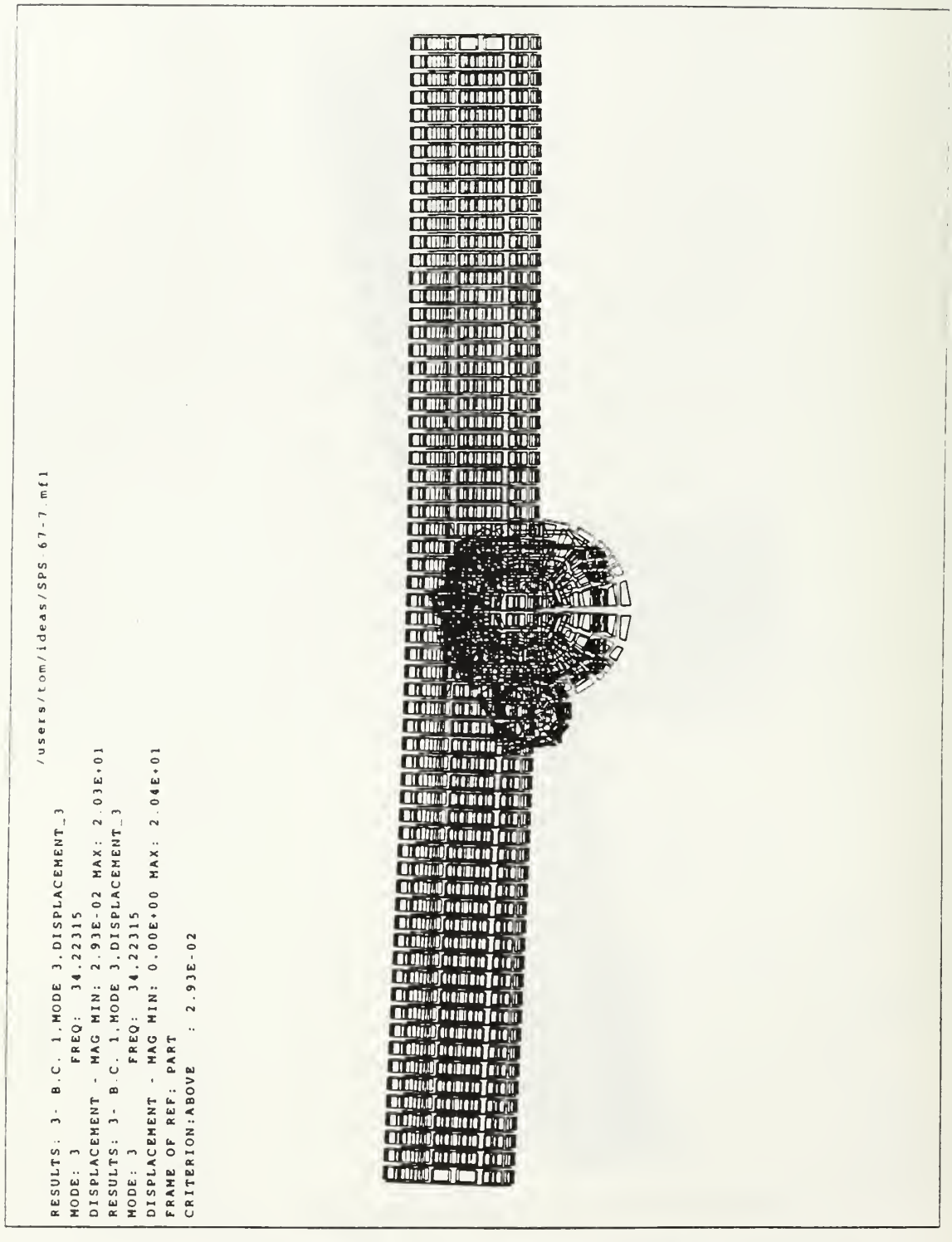

FIGURE 4.3: MODE 3 (TOP VIEW)

FIGURE 4.4: MODE 4 (FRONT VIEW)

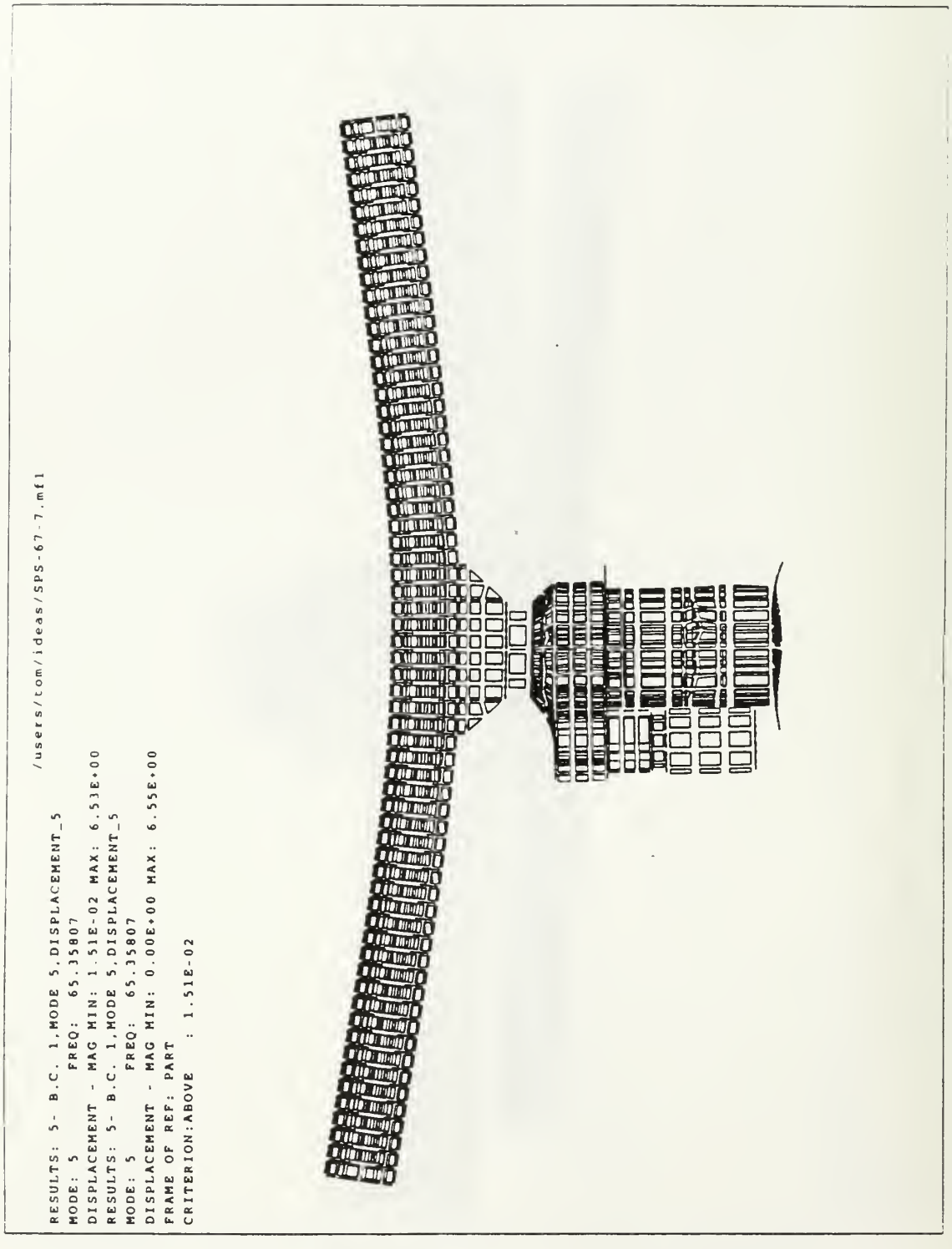

FIGURE 4.5: MODE 5 (FRONT VIEW)

FIGURE 4.6: MODE 6 (TOP VIEW)

FIGURE 4.7: MODE 7 (FRONT VIEW)

FIGURE 4.8: MODE 8 (FRONT VIEW)

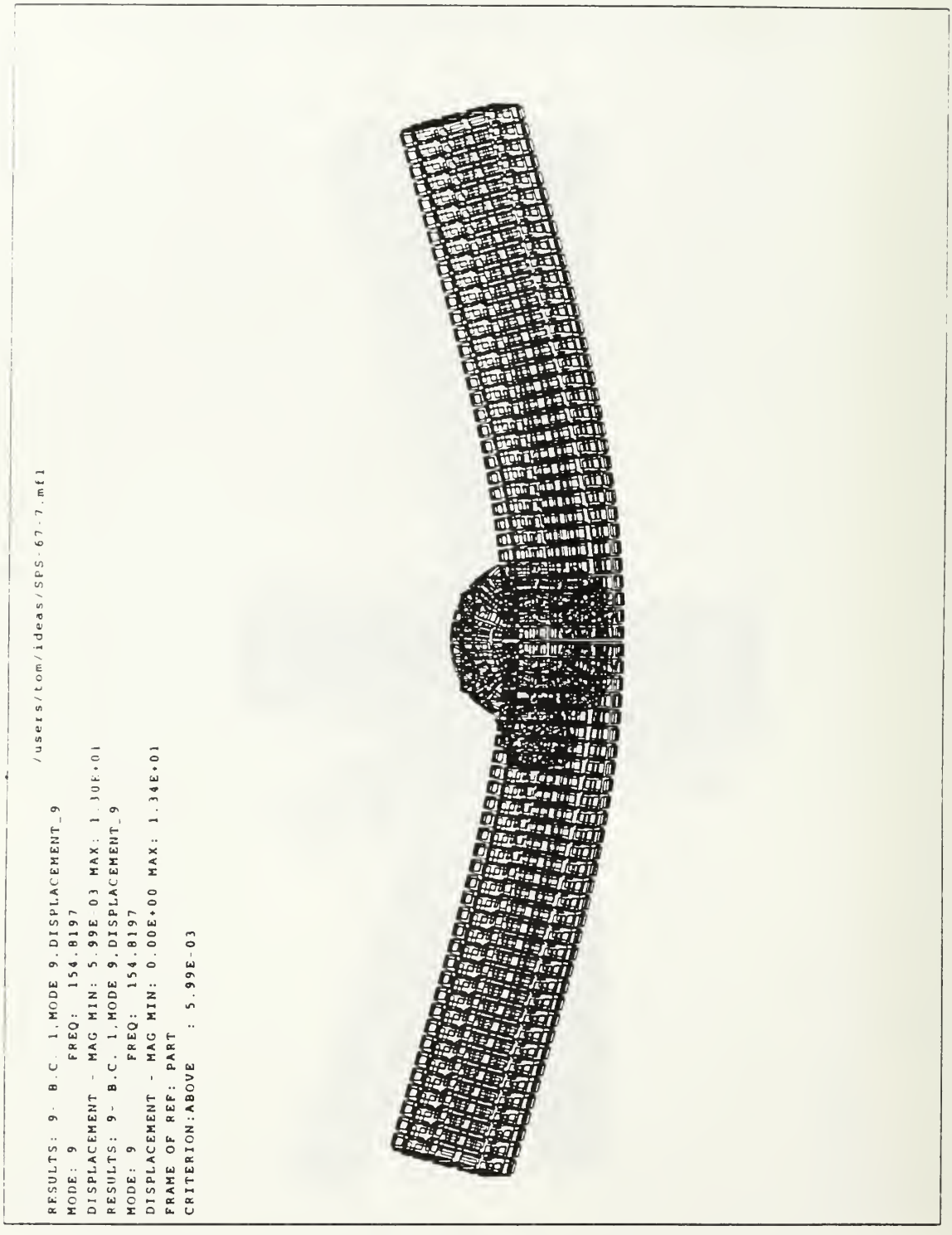

FIGURE 4.9: MODE 9 (TOP VIEW)

FIGURE 4.10: MODE 10 (FRONT VIEW)

FIGURE 4.11: MODE 11 (FRONT VIEW)

FIGURE 12: MODE 12 (FRONT VIEW)

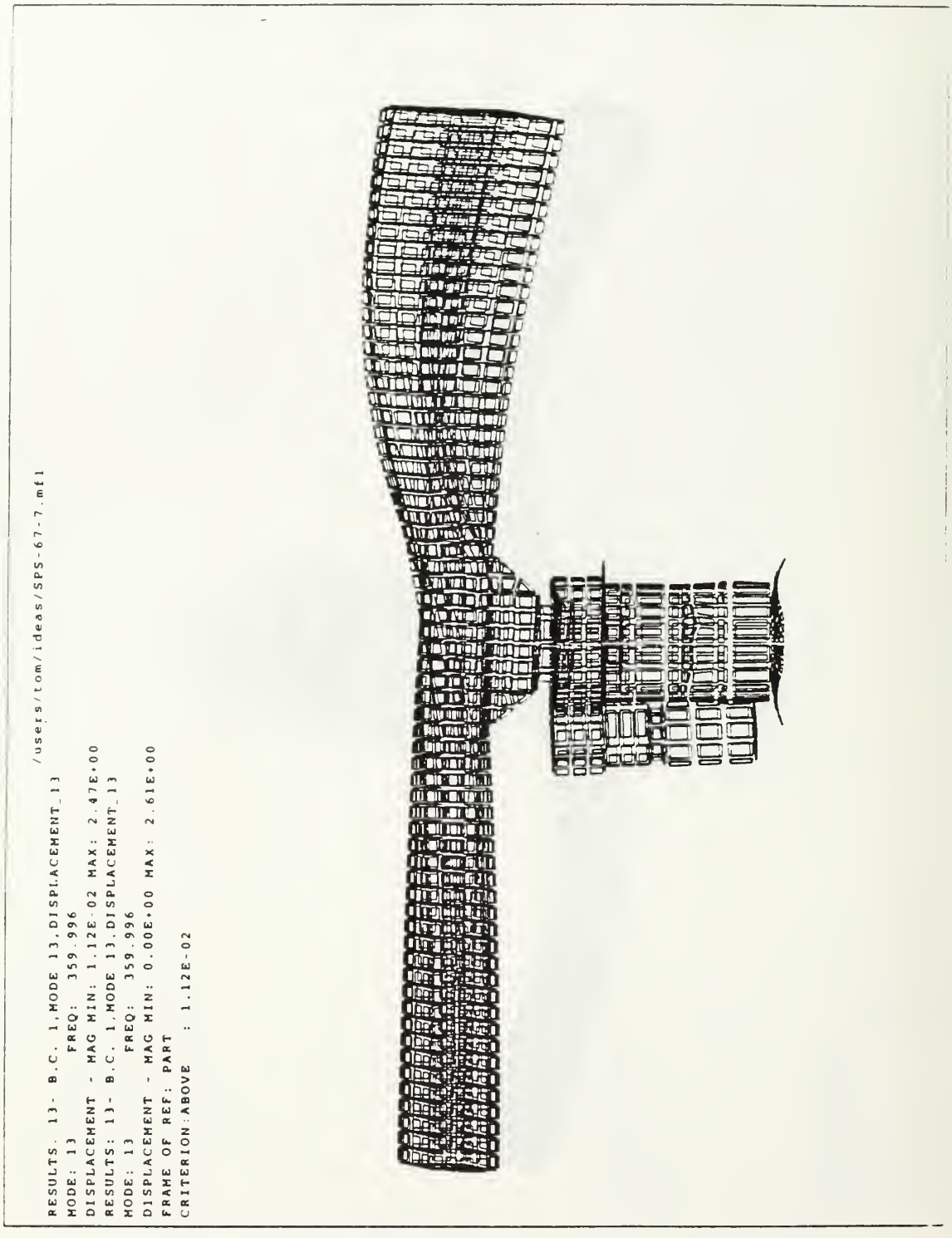

FIGURE 4.13: MODE 13 (FRONT VIEW)

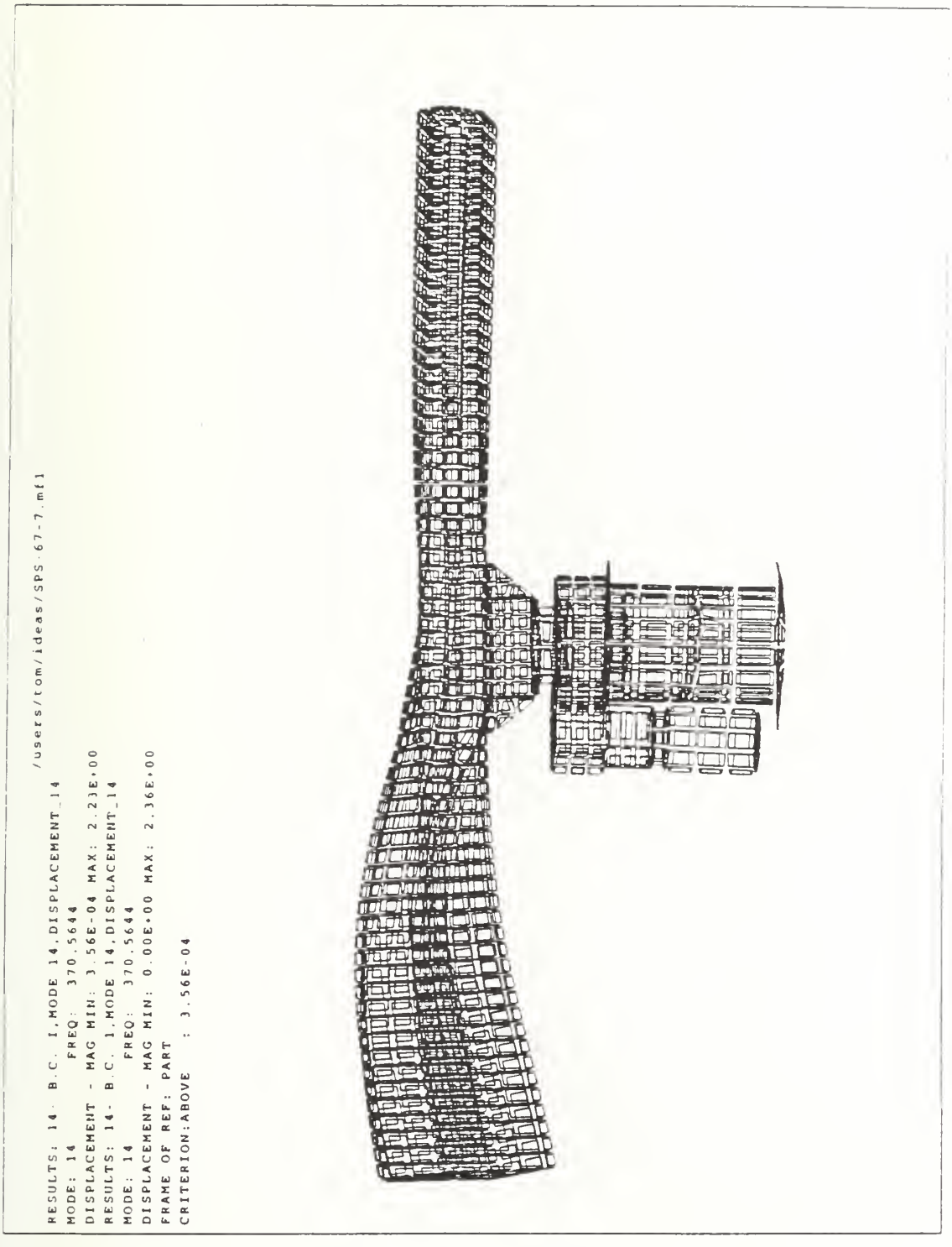

FIGURE 4.14: MODE 14 (FRONT VIEW)

FIGURE 4.15: MODE 15 (TOP VIEW)

FIGURE 4.16: MODE 16 (FRONT VIEW)

FIGURE 4.17: MODE 17 (FRONT VIEW)

FIGURE 4.18: MODE 18 (FRONT VIEW)

FIGURE 4.19: MODE 19 (FRONT VIEW)

FIGURE 4.20: MODE 20 (FRONT VIEW)

B. FREQUENCY RESPONSE ANALYSIS

I-DEAS evaluates a structure's response to applied excitations in Model Response. Model Response uses results from Model Solution. The normal modes are calculated and stored as a modal component model and then used to calculate the dynamic response.

Frequency response functions (FRF) provide a convenient basis for determining which modes are involved in the forced response of the antenna by providing insight into the frequency content of the computed responses. In order to calculate the FRF, the excitation and response must be measured. Once obtained, the absolute value of the ratio of response to excitation is plotted against its frequency. This yields the FRF for the test item.

In this study, three FRF were obtained, one for response of the antenna tip motion along each coordinate axis. To determine the FRF, the frequency of the enforced excitation is swept from low to high values. The FRF results in a series of peaks which are resonant with the normal modes of vibration of the antenna assembly. The height of the peaks depend upon the magnitude of excitation. The width of the peaks depend upon the damping value. A wider peak indicates higher damping.

Figure 4.21 is a FRF of the antenna assembly response along the x direction at the antenna tip. There is a multimode response involving the first mode at 16.82 Hz and

the second mode at 27.22 Hz. The first mode is much more excited than the second mode based on the height of the two peaks. This is expected since the first mode is the lateral roll mode, while the second mode is a yaw mode. No other modes appear to be excited.

Figure 4.22 is a FRF of the antenna assembly response along the y direction at the antenna tip. The mode that appears to be excited is the yaw mode at 27.22 Hz. This is the second mode and its motion is primarily in the horizontal plane.

Figure 4.23 is a FRF of the antenna assembly response along the z direction at the antenna tip. From the plot, it appears that the first mode at 16.82 Hz is being excited.

Comparison of these FRF with the Shock Qualification Test vibration plots, included in Appendix C, reveals a high degree of dynamic correlation between the finite element model and the test item.

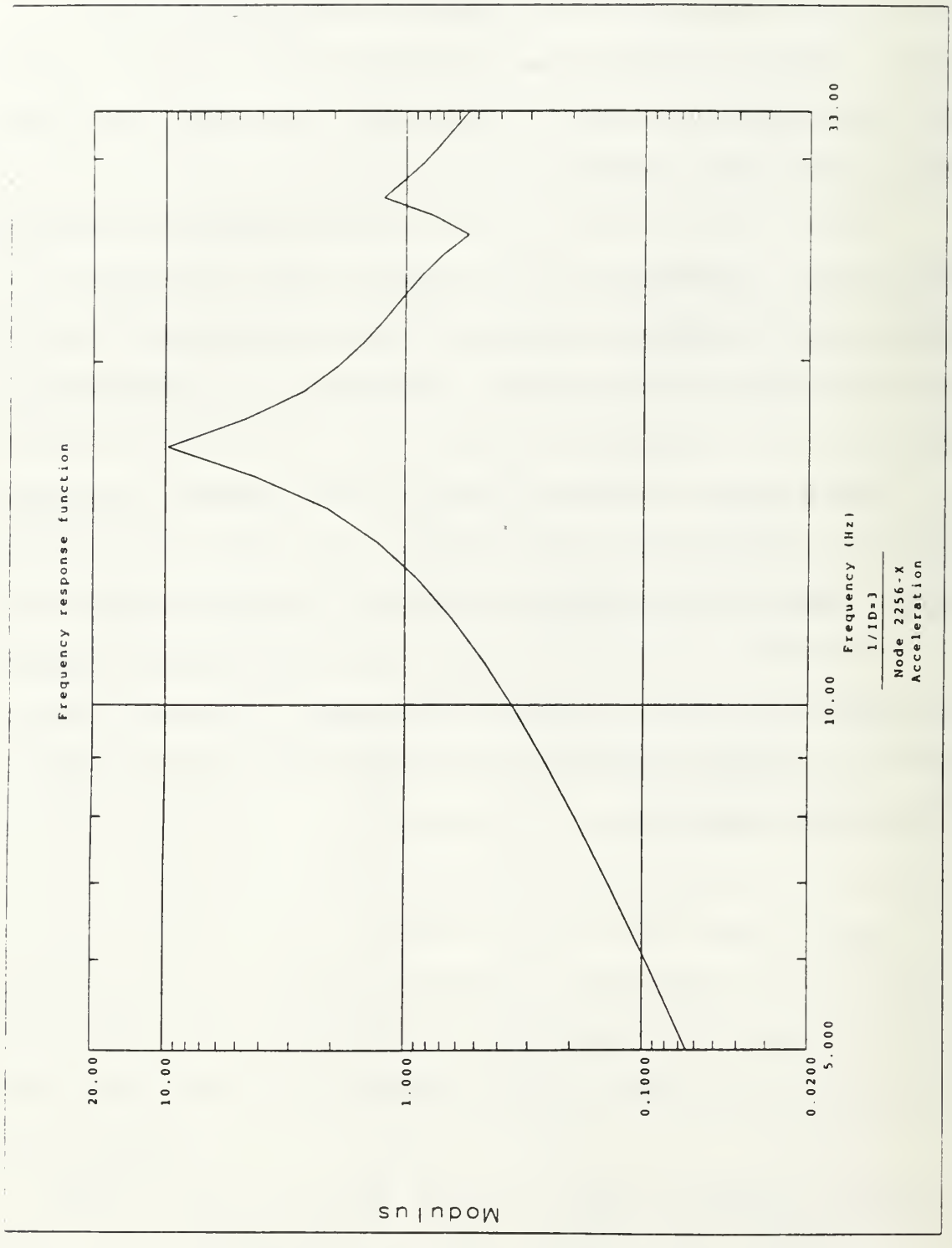

FIGURE 4.21: FREQUENCY RESPONSE FUNCTION (X DIRECTION)

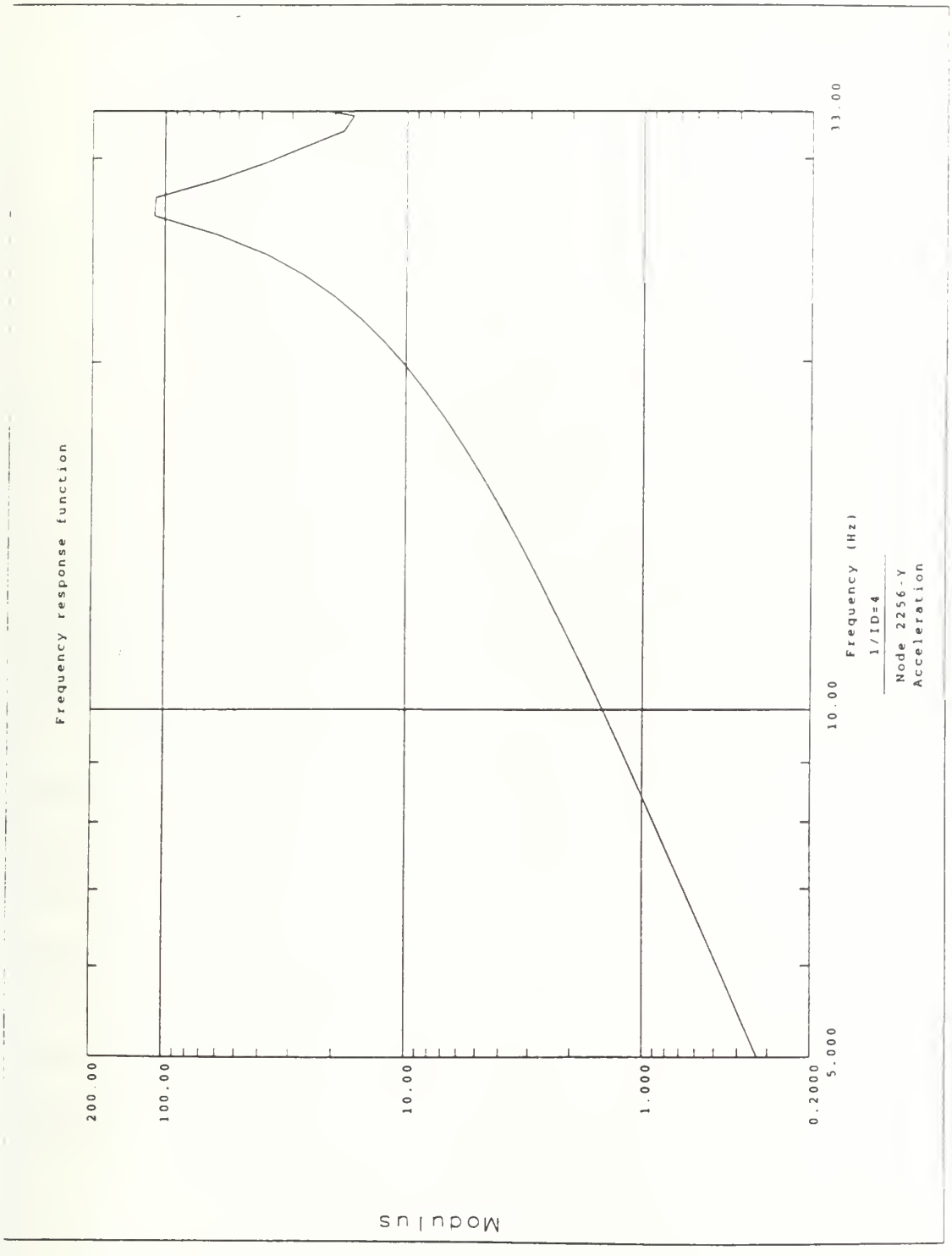

FIGURE 4.22: FREQUENCY RESPONSE FUNCTION (Y DIRECTION)

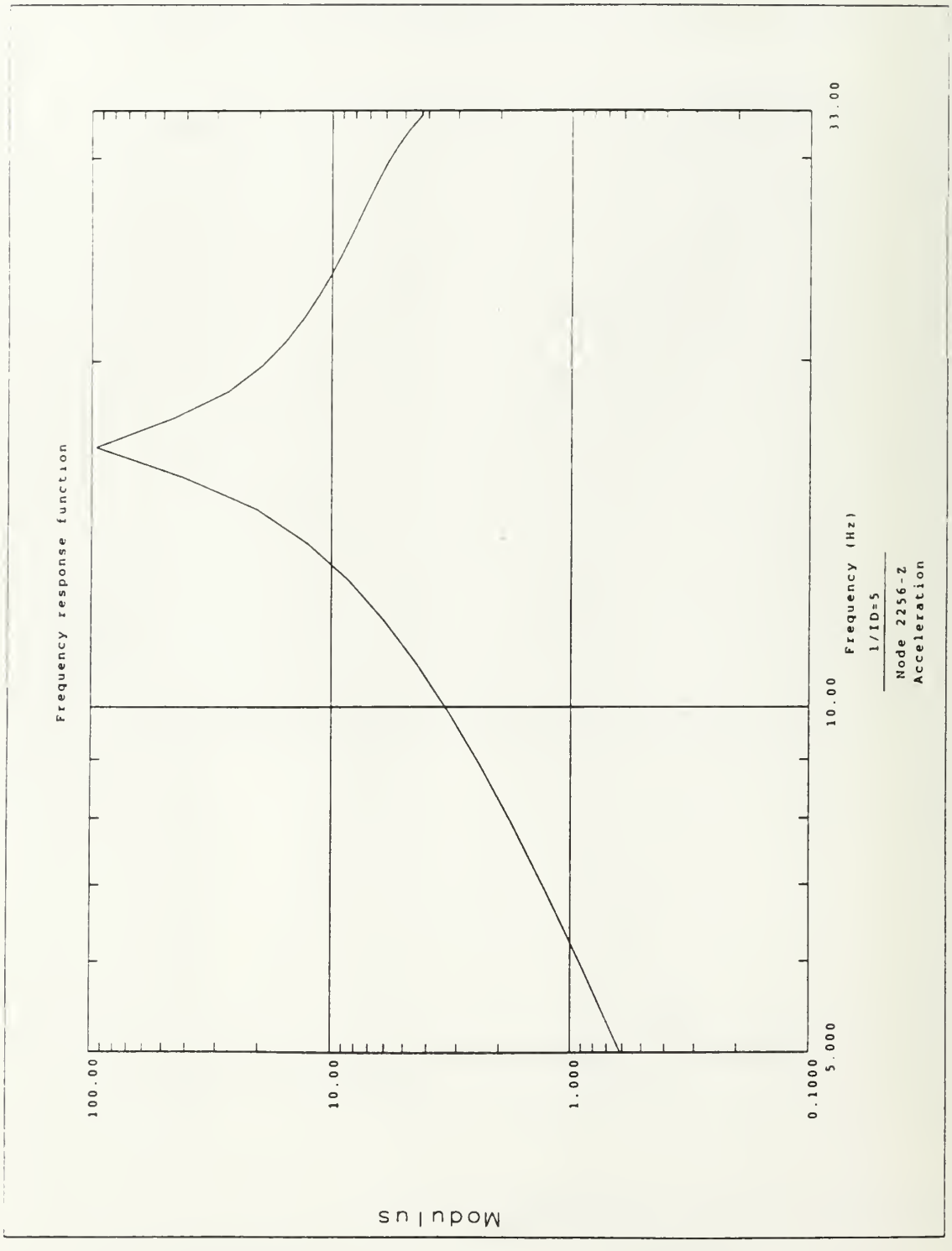

FIGURE 4.23: FREQUENCY RESPONSE FUNCTION (Z DIRECTION)

V. SUGGESTIONS FOR FUTURE WORK

A. TRANSIENT RESPONSE ANALYSIS

Once the normal mode and frequency response analyses of the antenna are performed, a transient response analysis of the antenna should be performed. The transient response analysis may be performed using excitation data from the Navy's Medium Weight Shock Machine (MWSM) and may be used to validate the finite element (FE) model. The excitation should be applied at the base of the pedestal in the form of a base acceleration. The resulting transient responses depend primarily on the system's natural frequencies, damping, and excitation force. If the base excitation frequencies are near the system's natural frequencies, resonance will occur, resulting in large deformations of the structure. The corresponding stresses and strains may be sufficient to cause failure. In order for the antenna to maintain its structural integrity, it must not fracture or crack when tested. The design must, therefore, ensure that the elastic limits of the materials used in construction of the antenna are not reached.

B. A MULTI–DEGREE OF FREEDOM SYSTEM SUBJECTED TO BASE EXCITATION

As an illustration of the transient shock analysis, consider the multi–degree of freedom system shown in Figure 5.1, with N physical DOF, damping matrix [C], stiffness matrix [M], and arbitrary time varying base excitation, $\{F(t)\}$.

The governing differential equation of motion for the NDOF system is :

$$[M]\{\ddot{q}(t)\} + [C]\{\dot{q}(t)\} + [K]\{q(t)\} = \{F(t)\} \tag{5.1}$$

The initial conditions of the system are given as:

$$\{q(t)=0\} = \{q_0\} \tag{5.2}$$

and

$$\{\dot{q}(t)=0\} = \{\dot{q}_0\} \tag{5.3}$$

The system can be transformed from physical coordinates to modal coordinates using the following transformation:

$$\{q(t)\} = [T]\{u(t)\} \tag{5.4}$$

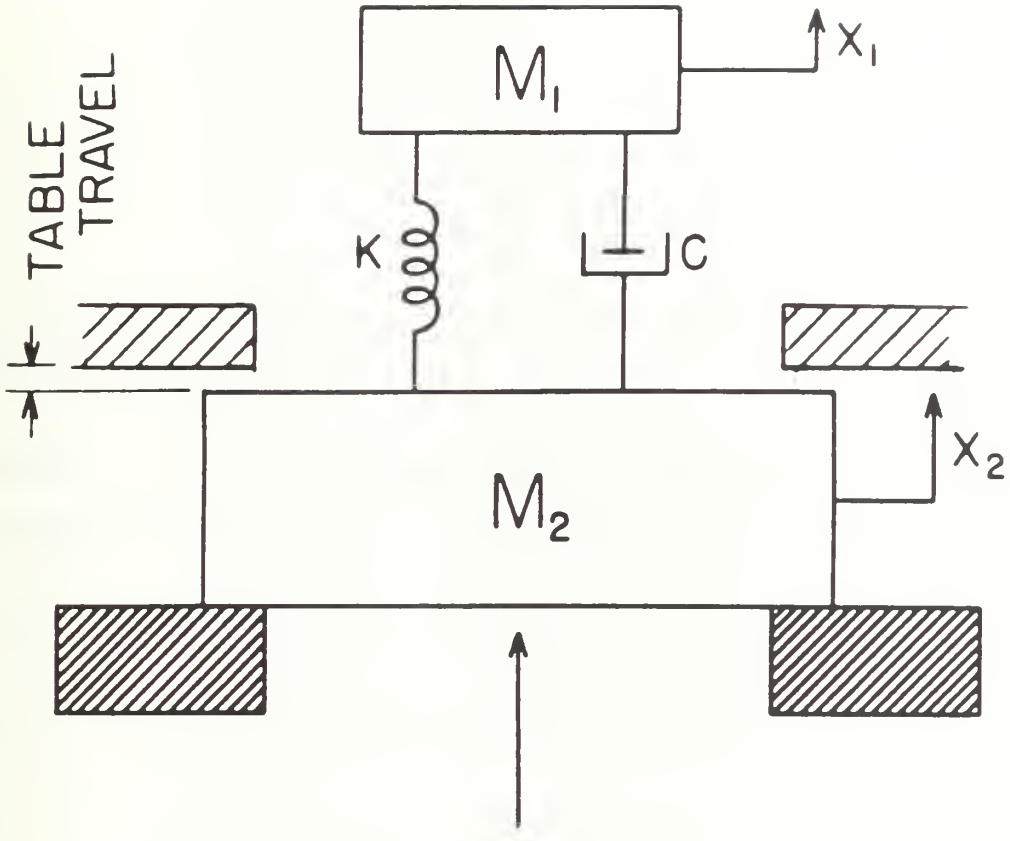

FIGURE 5.1: MDOF SYSTEM.

where

$$[T] = [\tilde{\Phi}]$$

and

$$\{x(t)\} = \sum_{i=1}^{N} \{\phi^i\}\{q(t)\}$$

The transformation matrix, $[\tilde{\Phi}]$, is the truncated modal matrix. The truncation results from the normal mode solution.

Substituting Equation (5.4) into Equation (5.3) yields a system of coupled second order ordinary differential equations:

$$[M][\tilde{\Phi}]\{\ddot{u}(t)\} + [C][\tilde{\Phi}]\{\dot{u}(t)\} + [K][\tilde{\Phi}]\{u(t)\} = \{F(t)\} \qquad (5.5)$$

Premultiplying Equation (5.5) by $[\tilde{\Phi}]^T$ yields:

$$[\tilde{\Phi}]^T[M][\tilde{\Phi}]\{\ddot{u}(t)\} + [\tilde{\Phi}]^T[C][\tilde{\Phi}]\{\dot{u}(t)\} + [\tilde{\Phi}]^T[K][\tilde{\Phi}]\{u(t)\} = [\tilde{\Phi}]^T\{F(t)\} \qquad (5.6)$$

Assuming proportional damping, the mass, damping and stiffness matrices are diagonalized resulting in N uncoupled second-order ordinary differential equations:

$$[M]\{\ddot{u}(t)\} + [C]\{\dot{u}(t)\} + [K]\{u(t)\} = \{f(t)\} \qquad (5.7)$$

where

$$[C] = \alpha[M] + \beta[K]$$

and

$$\{f(t)\} = \left[\tilde{\Phi}\right]^T \{F(t)\}$$

Dividing through by $[M]$ yields:

$$\{\ddot{u}(t)\} + \left[2\zeta_i\omega_i\right]\{\dot{u}(t)\} + \left[\omega_i^2\right]\{u(t)\} = \{a(t)\} \qquad (5.8)$$

where

$$\omega_i^2 = \frac{K_{ii}}{M_{ii}} \quad , \quad 2\gamma_i\omega_i = (\alpha_i + \beta_i\omega_i^2)$$

and

$$\{a(t)\} = \frac{1}{M}\{f(t)\}$$

Note: $\{a(t)\}$ is the artitrary time varying base acceleration.

The resulting single DOF equation of motion is:

$$\ddot{u}_i(t) + 2\gamma_i\omega_i\dot{u}_i(t) + \omega_i^2 u(t) = a_i(t) \qquad (5.9)$$

Having transformed the differential equation of motion into modal coordinates, we must transform the initial conditions as well:

$$\{q_0\} = [\tilde{\Phi}]\{u_0\} \tag{5.10}$$

and

$$\{\dot{q}_0\} = [\tilde{\Phi}]\{\dot{u}_0\} \tag{5.11}$$

Premultipying by $[\tilde{\Phi}]^T[M]$ yields:

$$[\tilde{\Phi}]^T[M]\{q_0\} = [\tilde{\Phi}]^T[M][\tilde{\Phi}]\{u_0\} \tag{5.12}$$

and

$$[\tilde{\Phi}]^T[M]\{\dot{q}_0\} = [\tilde{\Phi}]^T[M][\tilde{\Phi}]\{\dot{u}_0\} \tag{5.13}$$

Solving for $\{u_0\}$ and $\{\dot{u}_0\}$ yields:

$$\{u_0\} = [M]^{-1}[\tilde{\Phi}]^T[M]\{q_0\} \tag{5.14}$$

and

$$\{\dot{u}_0\} = [M]^{-1}[\tilde{\Phi}]^T[M]\{\dot{q}_0\} \tag{5.15}$$

Applying the transformed initial conditions to Equation (5.9) and solving, results in the following general solution:

$$u_i(t) = u_{i0}\cos\omega_i t + \frac{1}{\omega_i}\dot{u}_{i0}\sin\omega_i t + \frac{1}{\omega_i}\int_0^t a_i(t)\sin[\omega_i(t-\tau)]d\tau \qquad (5.16)$$

In order to solve for the physical displacements, x(t), transform back to physical coordinates using Equation (5.4):

$$\{q(t)\} = [\tilde{\Phi}]\{u(t)\}$$

C. HIGH IMPACT SHOCK TESTING OF SHIPBOARD SYSTEMS (MIL-S-901D)

The U.S. Navy currently has an extensive program to shock harden all surface ships. Ship shock tests are performed routinely on the lead ship of each class of ship as part of the ship's initial sea trials. Additionally, shock trials of ships of the same class are performed at the discretion of the Chief of Naval Operation (CNO) in order to validate upgrades of existing systems or new systems. All mission-essential items for installation aboard shock hardened ships must meet requirements outlined in Military Specification (MIL-S-901D), "Shock Tests, High Impact; Shipboard Machinery, Equipment and Systems, Requirements for" [Ref. 7]. These requirements establish the standards for all contracting activities upon which to base their shock testing criteria.

The AN/SPS-67(V)3 antenna assembly was shock tested on the Navy High Impact Shock Machine for Medium Weight Equipment (MWSM) shown in Figure 5.2. The shock test was completed without discrepancies on 31 August 1988 [Ref. 8]. The MWSM is used for shock qualification of equipment ranging in weight from 230 to 6000 lbs. The MWSM delivers high energy, high frequency shock to the anvil table from below by means of a 3000 lb hammer which swings through an arc of up to 270 degrees. The hammer height is adjusted in accordance with MIL-S-901D based upon the total weight on the anvil

table. The hammer strikes the 4500 lb anvil table imparting an upward, uniaxial acceleration to it. The anvil table is bolted to the MWSM foundation by 12 2—inch diameter bolts which permits the anvil table to travel up to 3 inches vertically upon hammer impact. Mission—essential items for installation aboard shock hardened ships are attached to the anvil table using a 60 by 60 inch mounting surface shown in Figure 5.3.

The AN/SPS—67(V)3 antenna assembly was attached to the Standard Mounting Fixture using eight (8), 3/4-10, Grade 5 bolts [Ref. 9]. MIL—S—901D mandates that test items be mounted in a manner characteristic of its normal shipboard orientation along with any foundation or supporting structure. Refer to Appendix C for antenna orientation and test setup. The AN/SPS—67(V)3 antenna assembly received six (6) shock blows at approximately 50 G's, 30 +/- 5 Hertz, with no discrepancies [Ref. 10]. Accelerometers were attached to the AN/SPS—67(V)3 antenna assembly to measure the shock excitation and equipment response. Refer to Appendix C for equipment data sheets.

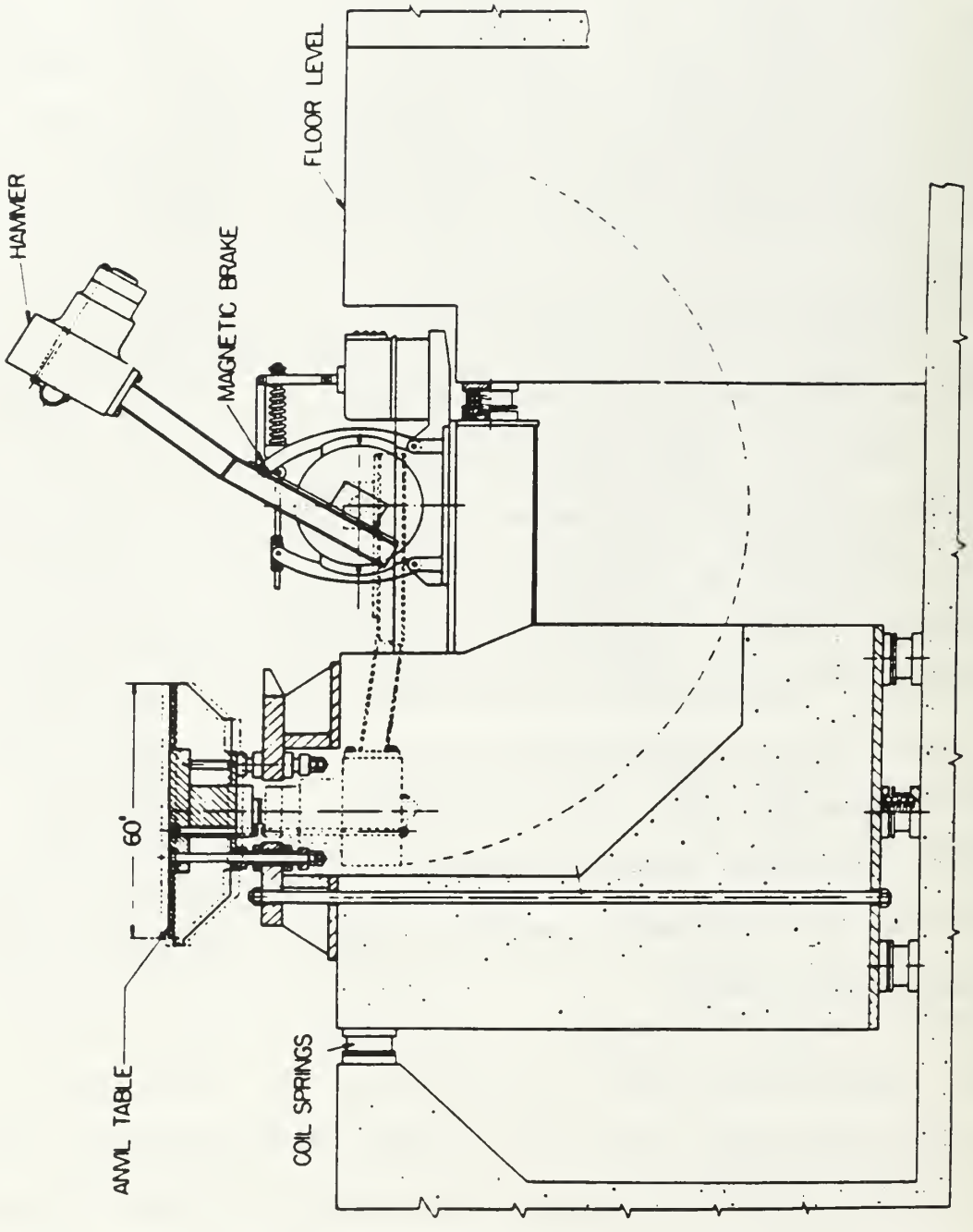

FIGURE 5.2: NAVY HIGH IMPACT SHOCK MACHINE FOR MEDIUM WEIGHT EQUIPMENT (MWSM). COURTESY CLEMENTS.

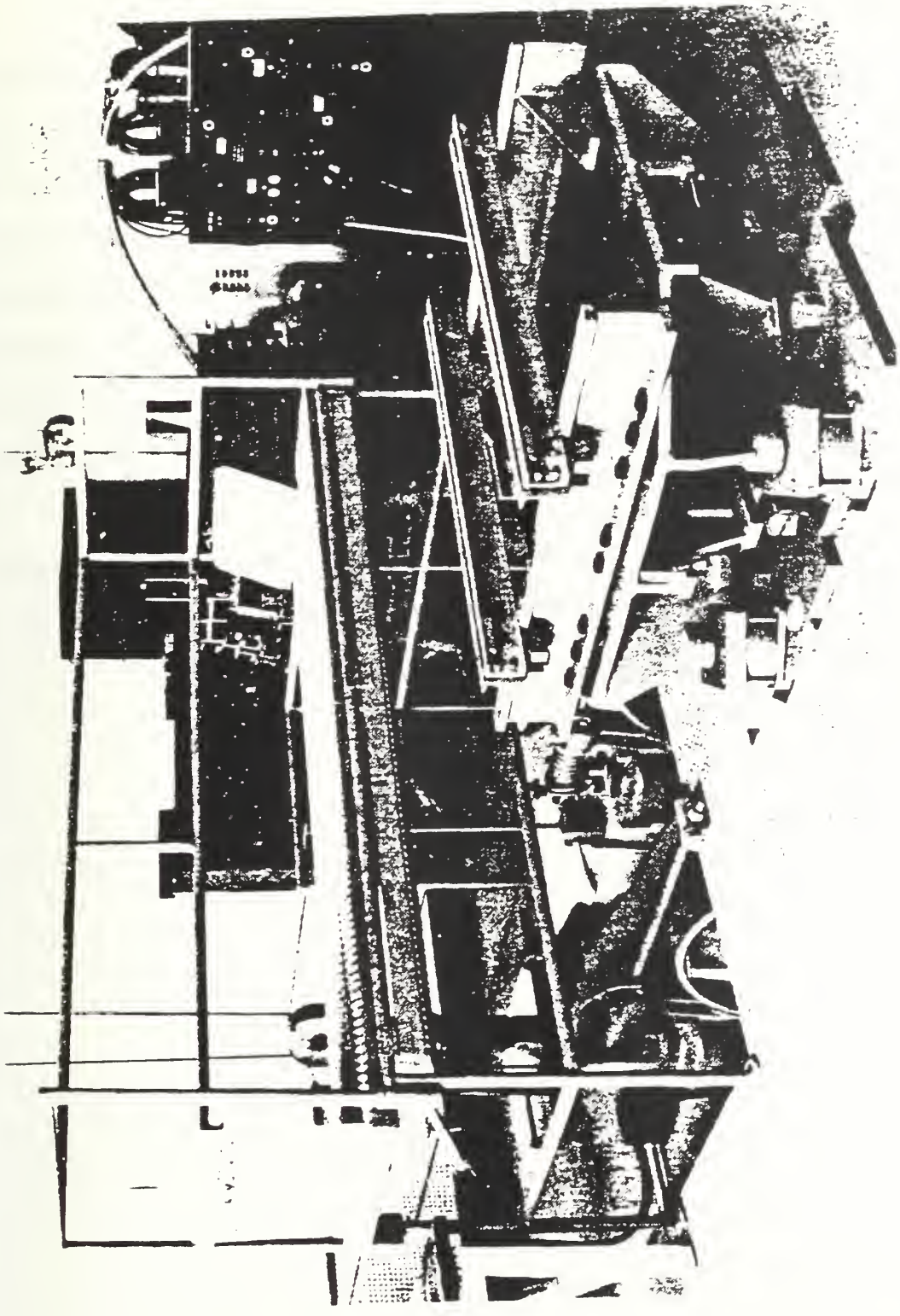

FIGURE 5.3: MWSM ANVIL TABLE AND STANDARD MOUNTING FIXTURE.

D. EXCITATION DEFINITION

The applied excitation used to perform the transient shock analysis is defined using the Excitation Definition Task. The excitation which is recommended for use may be described as a prescribed acceleration. The acceleration data was experimentally obtained from the MWSM and is included in Figure 5.4 [Ref. 11]. The excitation should be applied vertically to the 8 restrained nodes in the pedestal bottom plate which represent the antenna assembly bolt hole locations.

Damping is also defined using the Excitation Definition Task. Viscous damping should be assumed. A value of 0.02 is recommended for each normal mode.

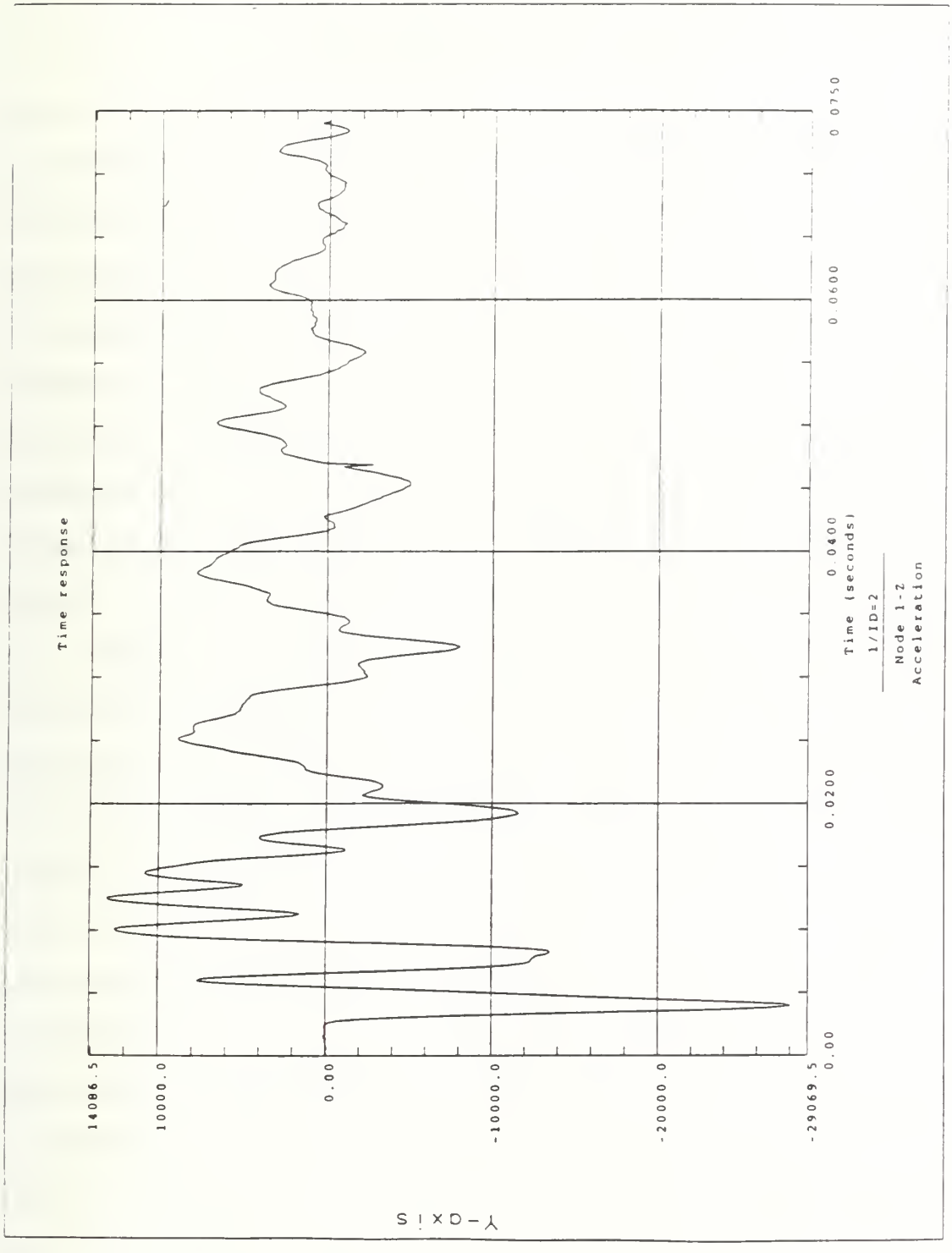

FIGURE 5.4: EXCITATION DEFINITION

VI. CONCLUSIONS

In an effort to shock harden U.S. Navy combatants, through the application of modern digital techniques, a NAVSEA-sponsored program is underway which will allow for the design of mast/antenna systems with optimal placement of antennae for maximum survivability of shipboard combat systems subjected to weapons effects. The program is focused on designing mast/antenna systems with as little dynamic amplification due to resonance as possible. These structural design considerations will have a significant impact on the combat effectiveness, i.e. the electromagnetic design, of U.S. Navy warships. Ultimately, a design which can accommodate these two very important considerations must be achieved. The finite element analysis is an efficient tool to study these considerations as it provides the engineer with a timely and inexpensive evaluation technique.

The primary goal of this study has been to construct an accurate finite element (FE) model of the AN/SPS-67(V)3 antenna assembly and to demonstrate the viability of its use for future live fire test and evaluation (LFT&E). This goal has been achieved.

This study initially gave a description of the AN/SPS-67(V)3 surface search radar system, a description of the underwater explosion (UNDEX) problem and the theoretical background associated with the solution of the normal modes of oscillation of the AN/SPS-67(V)3 antenna assembly. Next, a detailed description of the development of the AN/SPS-67(V)3 antenna assembly FE model was given. This description included discussion of the solid model representation of the antenna assembly and the mesh generation. Then, the response of the frequency response analysis at the antenna tip location was described, including a comparison of the FE response with the initial Shock Qualification Test vibration plots.

Comparison of the computed frequency response analysis responses with the Shock Qualification Test data show good agreement. The computed natural (resonant) frequencies from the AN/SPS-67(V)3 antenna assembly FE model were somewhat higher, by about 2 Hz, then those measured in the Shock Qualification Test. This difference may be the result of over-constraining the antenna pedestal at the bolt-hole locations and an under-estimate of the overall structural mass of the antenna assembly.

The most critical component in the design of the FE model representation of the AN/SPS-67(V)3 antenna assembly was the duplexed, radial contact ball bearings which provide support for the antenna sub-assembly while allowing it to

scan at antenna rotation speed, either 15 rpm or 30 rpm. Several different designs were solved and compared. The best design, involving the use of node-to-node translational and node-to-node rotational springs, was used in the final report. The effective bearing stiffnesses were computed based on the manufacture's free race analysis of the bearings. Eight symmetrically spaced nodal points were used. In order to refine the FE solution, more nodal points should be used, i.e. either sixteen or thirty-two.

After constructing the FE model of the antenna assembly and computing its normal modes of oscillation, the next step would be to validate the results with the modal test data obtained from a modal survey of the antenna assembly. The modal survey of the antenna assembly could not be completed prior to this study and the Shock Qualification Test data was used instead. This enabled comparison of natural frequencies of the antenna assembly but did not provide any insight into the associated mode shapes. Therefore, it is recommended that a modal survey of the antenna assembly be performed and the obtained modal parameters used to validate the computed mode shapes.

APPENDIX A. ANTENNA SUB—ASSEMBLY MODE SHAPES

The following plots are the mode shapes computed for the mesh comparison between the 3400 element mesh and the 2318 element mesh. There are 10 mode shapes listed in ascending order by frequency for the 2318 element mesh.

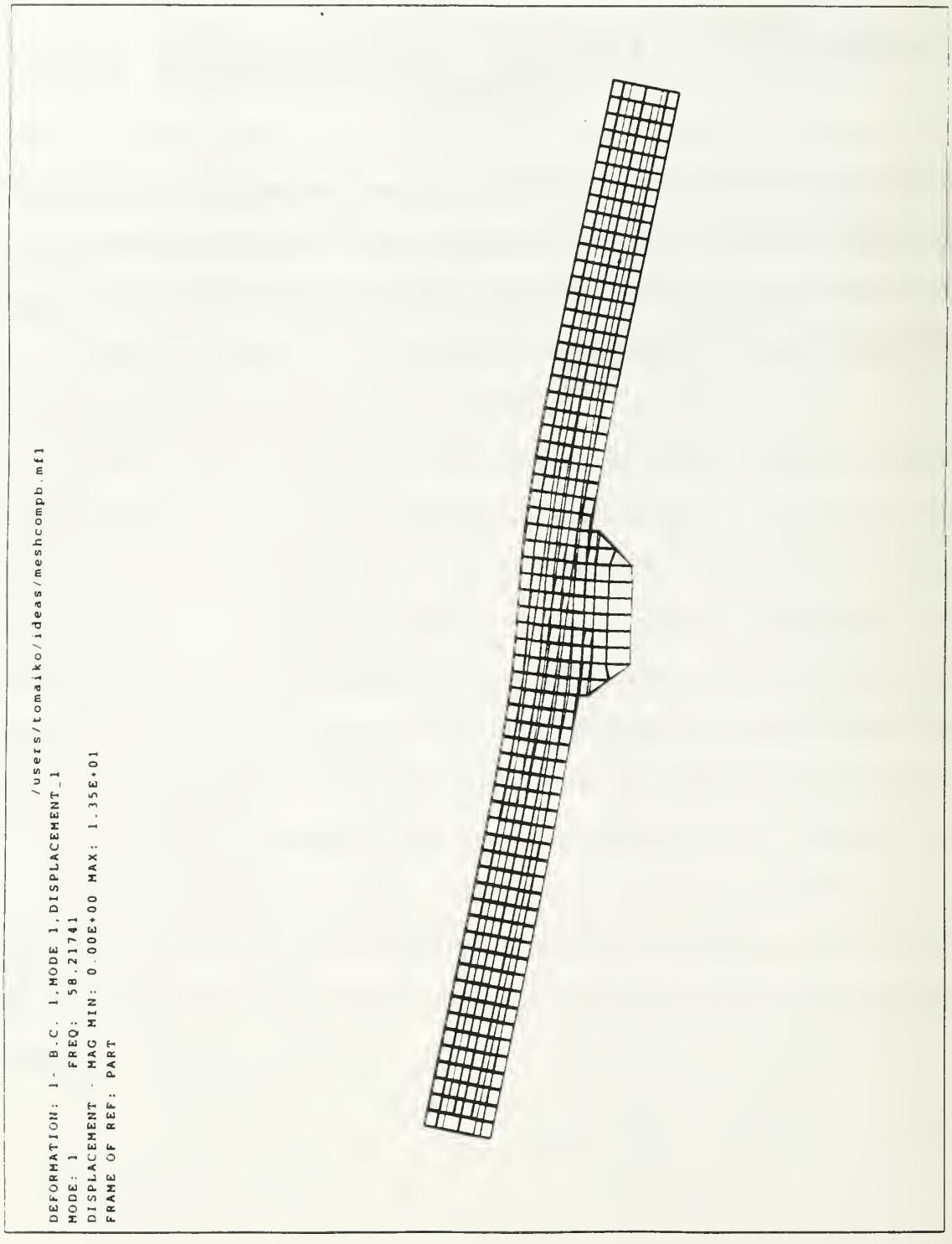

MODE 1 (FRONT VIEW)

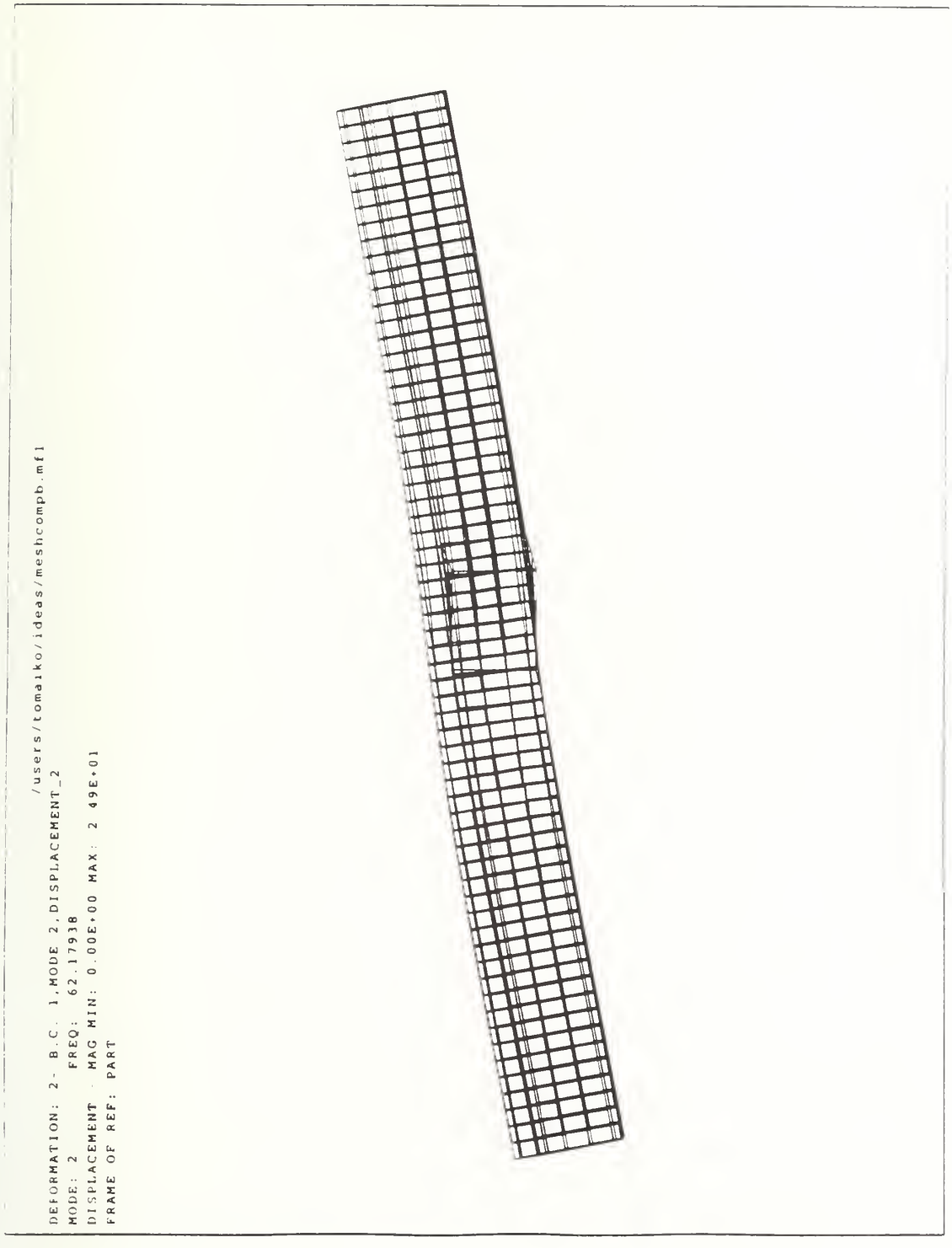

MODE 2 (TOP VIEW)

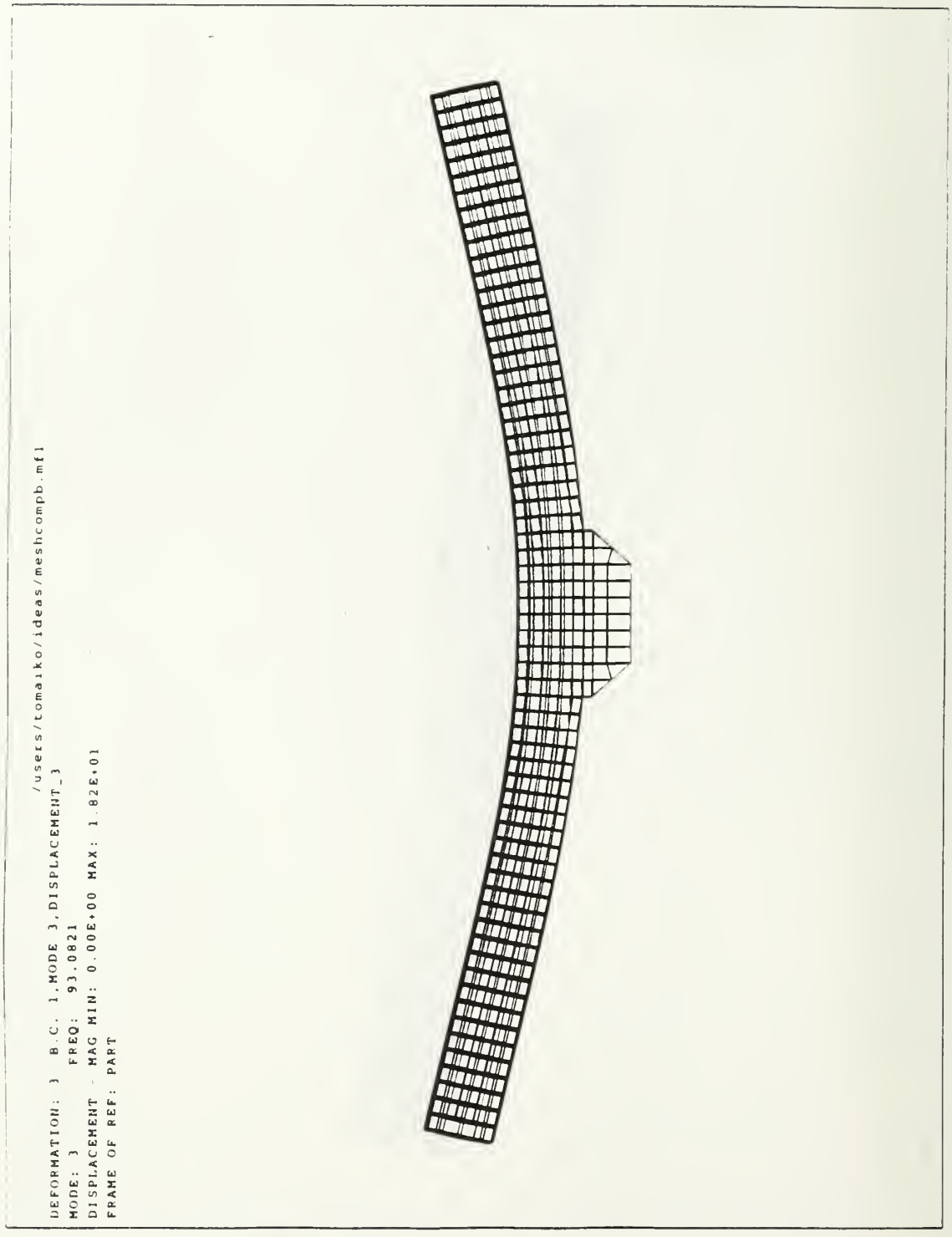

MODE 3 (FRONT VIEW)

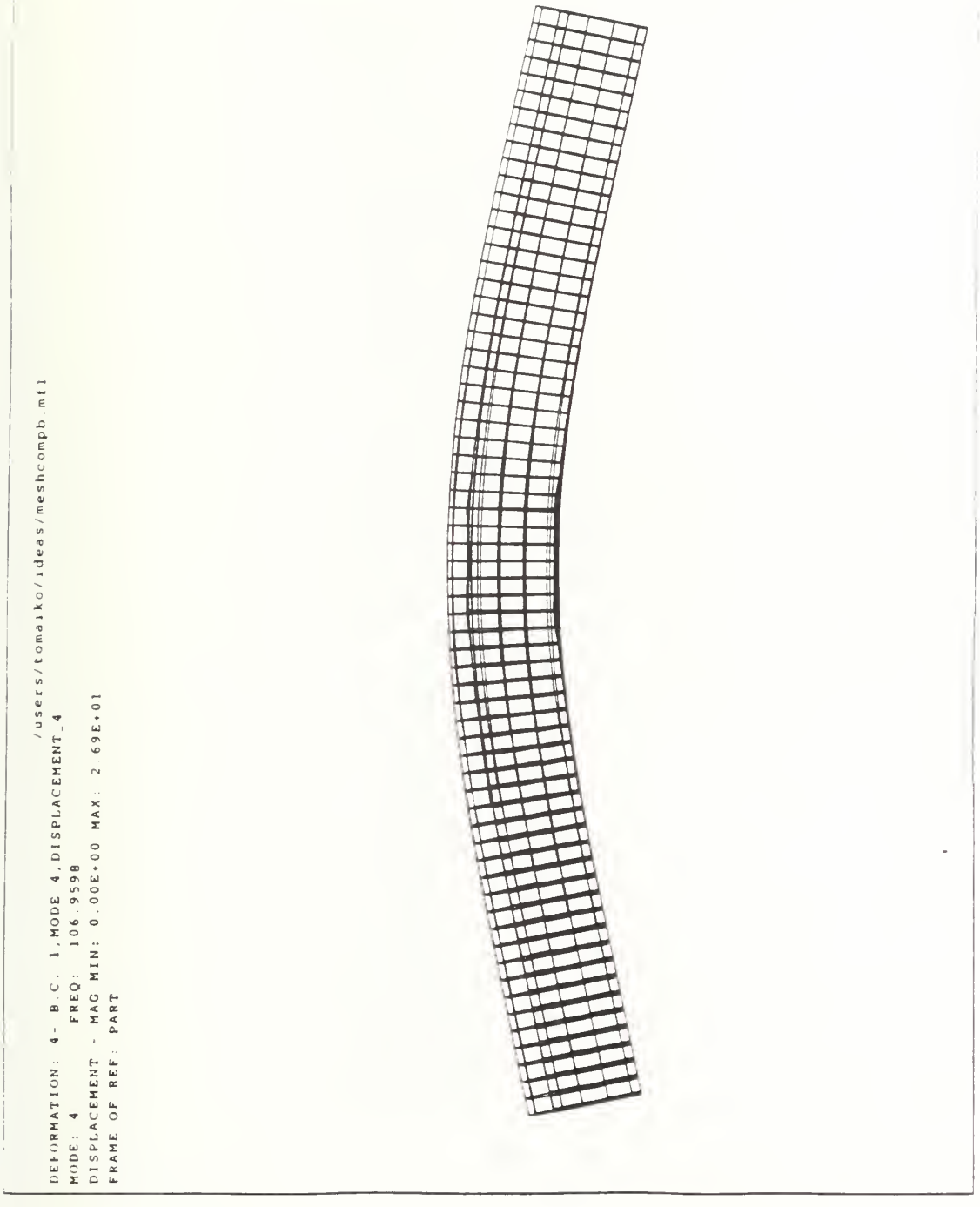

MODE 4 (TOP VIEW)

MODE 5 (FRONT VIEW)

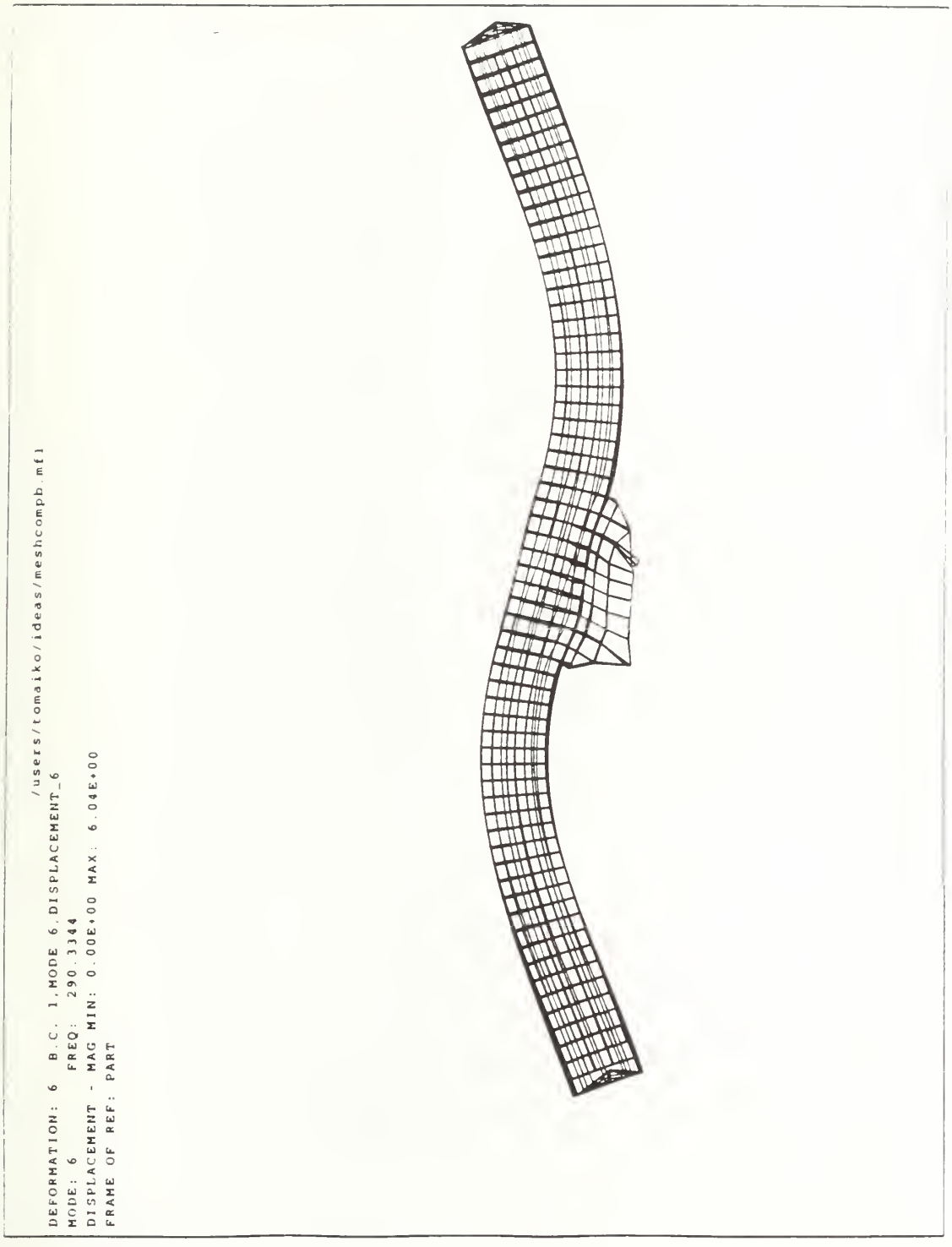

MODE 6 (FRONT VIEW)

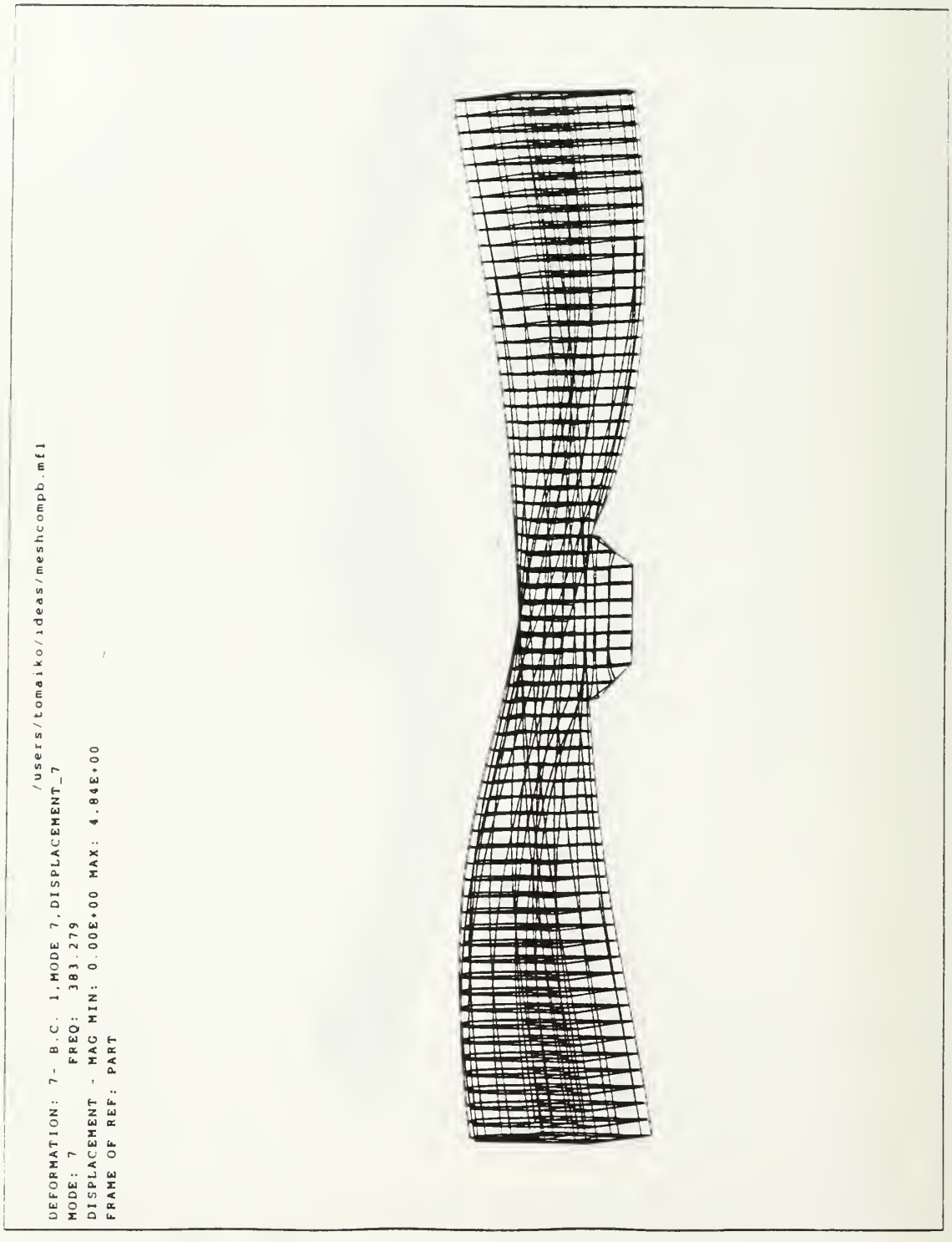

MODE 7 (FRONT VIEW)

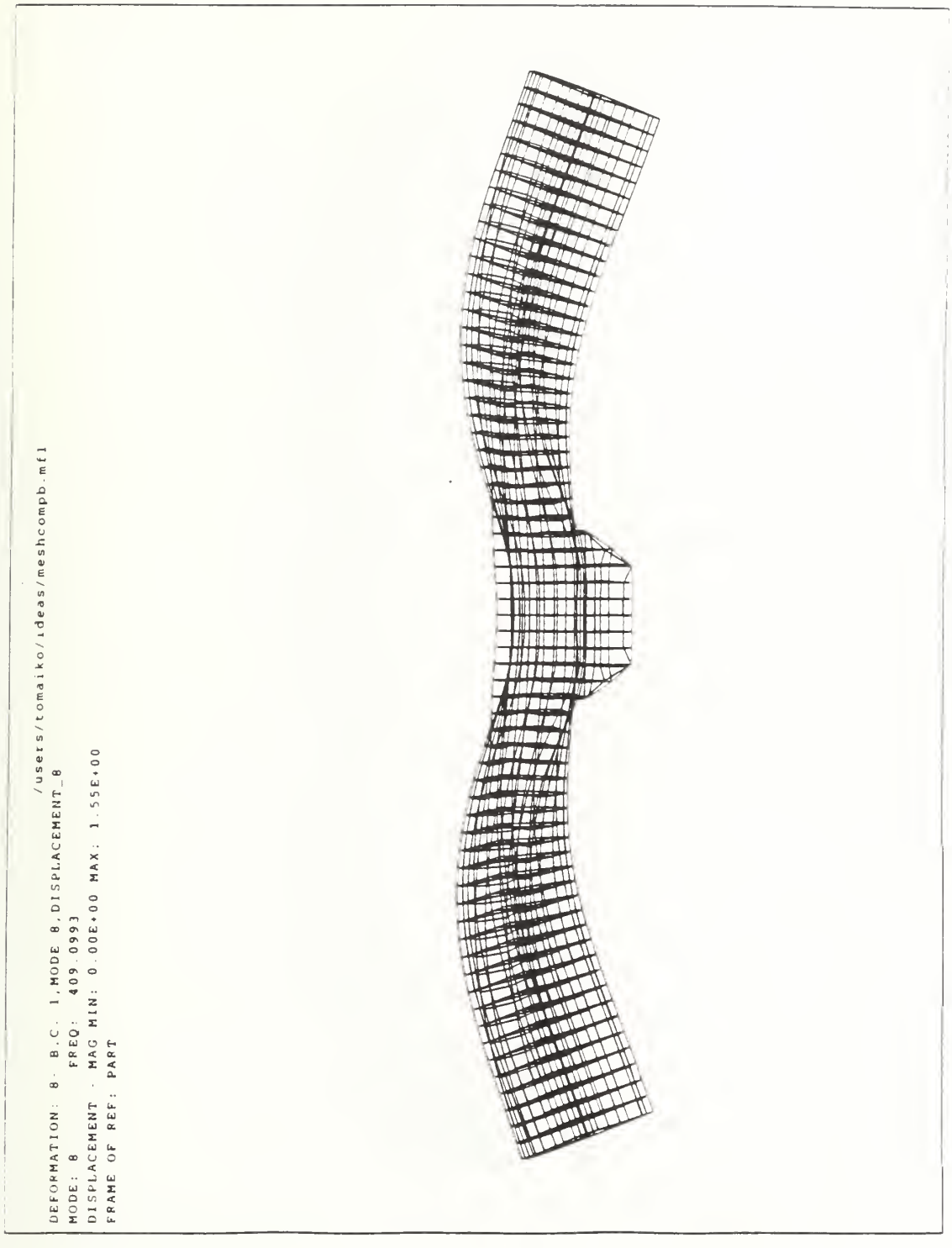

MODE 8 (FRONT VIEW)

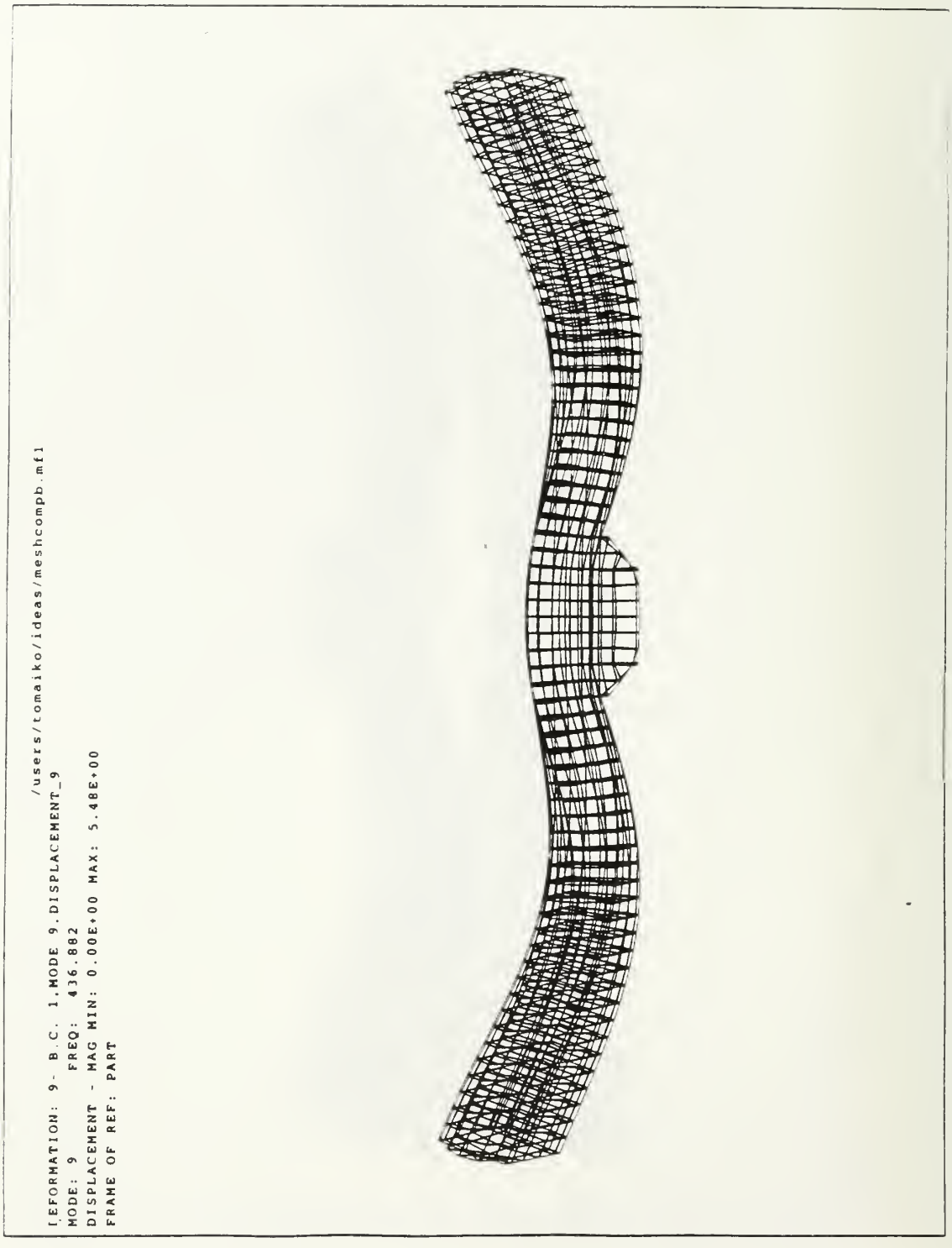

MODE 9 (FRONT VIEW)

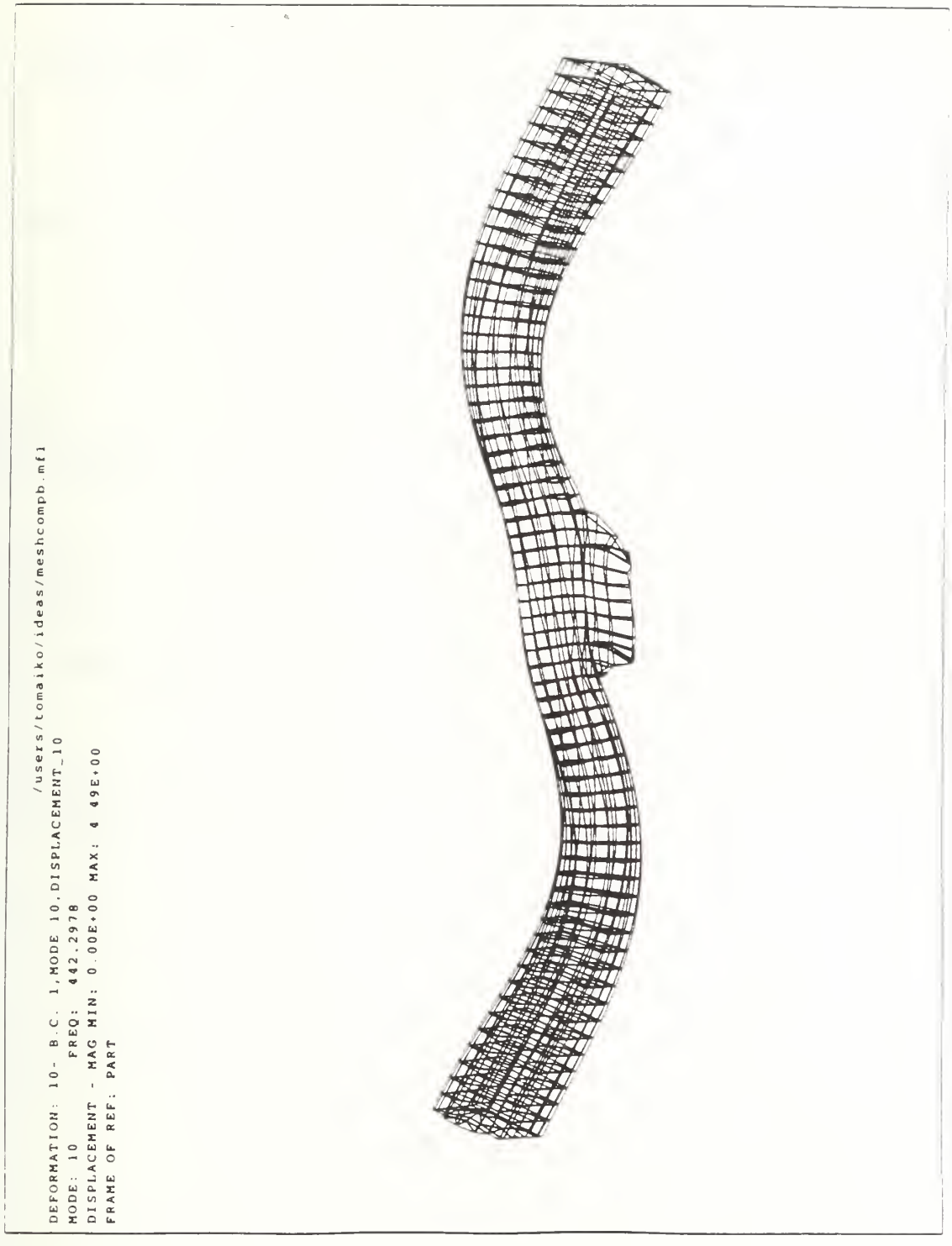

MODE 10 (FRONT VIEW)

APPENDIX B. MANUFACTURER'S BEARING ANALYSIS

The following is a manufacturer's free race analysis of the upper and lower duplexed, radial contact bearings.

KAYDON

FREE RACE RADIAL, AXIAL AND MOMENT STIFFNESS

CUSTOMER: NAVEL POST GRAD. SCHO
PROPOSAL NUMBER: N/A
BEARING NUMBER: 51532201

DATE: MARCH 24, 1994
ENGINEER: KEN SIPE
LOCATION: MUSKEGON, MI 49443

INPUT DATA:	DIAMETER	THICKNESS	WIDTH	MOD OF ELASTICITY
INNER RACE	6.00000	0.371	1.000	30000000
OUTER RACE	8.00000	0.325	1.000	30000000

CONTACT ANG	PD	BALL DIA	B-QTY	APL GAP	SPACING	MOUNTING
30	7.000	0.50000	28	0.00050	1.000	BACK-TO-BACK

RESULTS:
PRELOAD GAP AFTER INSTALLATION = 0.000500 IN
AXIAL PRELOAD AFTER INSTALLATION = 130 LB
PRELOAD CONTACT ANGLE = 30.413

RADIAL STIFFNESS = 2.59E6 LB/IN
RELIEF LOAD = 321 LB

AXIAL STIFFNESS = 1.32E6 LB/IN
RELIEF LOAD = 330 LB

MOMENT STIFFNESS = 2.01E7 IN-LB/RAD
RELIEF MOMENT = 1436 IN-LB

KAYDO

FREE RACE RADIAL. AXIAL AND MOMENT STIFFNESS

CUSTOMER: NAVAL POST GRAD SCHOO
PROPOSAL NUMBER: N/A
BEARING NUMBER: 51531201
DATE: MARCH 24, 1994
ENGINEER: KEN SIPE
LOCATION: MUSKEGON, MI 49443

INPUT DATA:	DIAMETER	THICKNESS	WIDTH	MOD OF ELASTICI
INNER RACE	4.50000	0.277	0.750	30000000
OUTER RACE	6.00000	0.277	0.750	30000000

CONTACT ANG	PD	BALL DIA	B-QTY	APL GAP	SPACING	MOUNTI
11	5.250	0.37500	42	0.00005	0.750	BACK-TO-

RESULTS:
PRELOAD GAP AFTER INSTALLATION = 0.000050 IN
AXIAL PRELOAD AFTER INSTALLATION = 0 LB
PRELOAD CONTACT ANGLE = 11.040

RADIAL STIFFNESS = 7.18E5 LB/IN
RELIEF LOAD = 2 LB

AXIAL STIFFNESS = 4.00E4 LB/IN
RELIEF LOAD = 1 LB

MOMENT STIFFNESS = 4.77E5 IN-LB/RAD
RELIEF MOMENT = 5 IN-LB

APPENDIX C. SHOCK QUALIFICATION TEST REPORT

The following is an excerpt from the antenna shock test report.

ENCLOSURE 4.13-4

ANTENNA GROUP SHOCK TEST REPORT

THIS ENCLOSURE CONSISTS OF 53 PAGES

TEST REPORT
ON
UNITED TECHNOLOGIES, NORDEN SYSTEMS, INC.
ANTENNA including PEDESTAL
OE-374/SPS-67

TEST REPORT NO: 7667-1-3835

REPORT WRITER: J. Czereuta
J. CZEREUTA

TEST ENGINEER: W.F. Ferry
W.F. FERRY

APPROVED BY: for DATE: 10-12-88
J.A. DEO, MANAGER
ENVIRONMENTAL LABORATORY
LOCKHEED ELECTRONICS CO., INC.
1501 US Hwy 22, C.S. #1
PLAINFIELD, NJ 07061-1501
U.S.A.

PURPOSE OF TEST:	The purpose of this test was to subject the Tes Item to the shock test requirements as specified in Purchase Order No:78-00P3396-ES, in accordance with Procedure TP177230-1.
TEST ITEM:	Description: ANTENNA including PEDESTAL OE-374/SPS-67
MANUFACTURER:	United Technologies, Norderm Systems, Inc. Norden Place Norwalk, CT 06856
APPLICABLE DOCUMENTS:	United Technologies, Norden Systems, Inc. Purchase Order No:78-00P3396-ES, dated 19 JUL 88. Procedure: TP177230-1.
PROJECT NUMBER:	G4-8031-4835
CONTRACT NUMBER:	N00024-79-C-7262
QUANTITY OF TEST ITEMS:	One (1) Antenna & Pedestal
SECURITY CLASSIFICATION OF TEST ITEMS:	Unclassified.
TEST CONDUCTED BY:	Lockheed Electronics Co., Inc. Environmental Laboratory 1501 U.S. Hwy 22, C.S. #1 Plainfield, NJ 07061-1501
DATE TESTS COMPLETED:	: 31 AUG 88.
DISPOSITION OF TEST ITEM:	Returned to United Technologies, Norden Systems, for post shock test and/or inspection.
SHIPPING DOCUMENTS:	LEC Packing Slip No.48532, dated 6 SEP 88.
ABSTRACT:	The Test Item was subjected to the shock test requirements specified in Purchase Order No.78-00P3396-ES, in accordance with TP177230-1. Shock was completed without discrepancies.

Refer to the test results section for additional information.

TEST APPARATUS: The following equipment was used in the performance of this test:

Medium-weight Shock Machine; New England Trawler Equipment Co. Model 10-T-3351-C; EL002.

Standard Mounting Fixture Fig. 9-1 & 10-1, of MIL-S-901C.

Torque Wrench; Armstrong; Model 64-104; S/N. R4393;
Cal:4/19/88; Due:10/21/88

Charge Amp Power Supply; Endevco; Model 4222; EL393;
Cal:8/30/88; Due:8/30/89.

Analyzer; Spectral Dynamics; Model SD375; EL030;
Cal:3/15/88; Due:9/15/88.

Band Pass Filter; Krohn-Hite; Model 330-M; EL534;
Cal:Functional.

Accelerometer Simulator; Endevco; Model 4815A; EL603;
Cal:7/7/88; Due:1/7/89.

X-Y Plotter; Hewlett-Packard; Model 7475A; EL603A;
Cal:Functional.

Accelerometers; Endevco;
Model 2225;
EL542; Cal:2/19/88; Due:2/19/89,
EL562A; Cal:2/19/88; Due:2/19/89,
EL300A; Cal:2/19/88; Due:2/19/89,
EL339A; Cal:2/19/88; Due:2/19/89,
Model 2224C;
EL606; Cal:3/3/88; Due:3/3/89,
EL605; Cal:3/3/88; Due:3/3/89.

Power Supply/Charge Amps; Endevco;
Model 2721B (1-5); EL393; Cal:8/30/88; Due:8/30/89,
Model 2721A (6); EL393; Cal:8/30/88; Due:8/30/89.

CALIBRATION: Unless noted otherwise, all test facilities and associated test equipment utilized in conducting tests specified herein, were calibrated in accordance with MIL-STD-45662.

TEST PROCEDURE:

The Test Item was attached to the test fixture using eight (8), 3/4-10, Grade 5 Bolts. The entire assembly was then secured to the medium-weight shock machine and subjected to the test requirements in accordance with TP177230-1, as outlined herein:

Refer to photo Figs.1 thru 6 for typical test setups.

Accelerometers were attached to the Test Item to monitor input and responces. Refer to Appendix A for data sheet information.

Prior to shock, a dummy load was used to simulate the weight of the Test Item, on the shock machine, a shock pulse of approximately 50G's, 30 +/-5Hz, was established.

Six (6) shock blows were applied at approximately 50 G's, 30 +/-5Hz with the following parameters:

FIG.9-1

BLOW	HAMMER HEIGHT	TABLE TRAVEL	ANTENNA ORIENTATION
1	12"	3"	Antenna parallel to mounting rails.
2	12"	3"	Antenna perpendicular to mounting rails.
3	12"	3"	Antenna rotating.

FIG.10-1

BLOW	HAMMER HEIGHT	TABLE TRAVEL	ANTENNA ORIENTATION
4	12"	3"	Antenna perpendicular to mounting rails.
5	12"	3"	Antenna 45 degrees from Blow #4.
6	12	3	Antenna parallel to mounting rails.

After each shock blow the Test Item was visually inspected for evidence of any discrepancies.

TEST RESULTS: Six (6) shock blows were completed with no discrepancies.

Refer to Factory Test Record, pg.6, and Appendix A, for additional information.

Photo pp.7 & 8.

RECOMMENDATIONS: None, data supplied for information only

FACTORY TEST RECORD
CLASS HI SHOCK
DAVIDS-0370 (REV. 12-48)

Issued by the Navy Department, Washington, D. C.
To be used in connection with Military Specifications MIL-S-901, MIL-T-945 and MIL-T-17113.

DATE: 8/31/88

TEST NO.: 7667-1-3835

1. ITEM NAME OF EQUIPMENT SHOCK-TESTED: ANTENNA AND PEDESTAL OE-374/SPS-67

2. RATING (HP, VOLTS, RPM, CPM, ETC.)

3. MAJOR PARTS

	MANUFACTURED	ADDRESS	GOV. DWG. NO.	IDENTIFYING NUMBER
PUMP, ETC. ANTENNA - PEDESTAL.	UNITED TECHNOLOGIES NORDEN SYSTEMS INC.	NORDEN PL. NORWALK, CT 06856.		
MOTOR, ETC.	MANUFACTURED	ADDRESS	GOV. DWG. NO.	IDENTIFYING NUMBER
STARTER, ETC.	MANUFACTURED	ADDRESS	GOV. DWG. NO.	IDENTIFYING NUMBER
4. CONTRACT NO.	CONTRACTOR	ADDRESS		

5. TYPE OF SHOCK TEST (INDICATE): [X] ASSEMBLY [ ] SUB-ASSEMBLY [ ] PART

6. TOTAL WEIGHT OF ASSEMBLY TESTED: TEST ITEM 428 LBS.

WEIGHT OF INDIVIDUAL MAJOR PARTS (Compressor, etc.) _____ LBS. MOTOR (Etc.) _____ LBS. STARTER (Etc.) _____ LBS

7. WEIGHT CLASSIFICATION OF ITEM (Indicate): [ ] LIGHT [X] MEDIUM

8. APPLICABLE MOUNTING FIGURE IN SPECIFICATION MIL-S-901 (Indicated): [ ] Fix. 4A Fig. 5 [ ] Fix. 4C Fig. 6 [X] Fig. 9-1 [X] Fig. 10-1 [ ] Fig. 10-2 [ ] OTHER (Specify)

9. FOR LIGHTWEIGHT ITEMS

FIRST CONDITION				SECOND CONDITION			
BLOW NO	DROP IN FEET	AXIS	DAMAGE INCURRED	BLOW NO	DROP IN FEET	AXIS	DAMAGE INCURRED
	1	BACK			1	BACK	
	3	BACK			3	BACK	
	5	BACK			5	BACK	
	1	TOP			1	TOP	
	3	TOP			3	TOP	
	5	TOP			5	TOP	
	1	SIDE			1	SIDE	
	3	SIDE			3	SIDE	
	5	SIDE			5	SIDE	

ITEMS SUBJECTED TO ABOVE TWO CONDITIONS WERE: [ ] SAME [ ] DISSIMILAR

REMARKS

E-1

10. FOR MEDIUM-WEIGHT ITEMS (Hammer Drop)

BLOW NO	GROUP NO	HAMMER DROP	DAMAGE INCURRED	BLOW NO	GROUP NO	HAMMER DROP	DAMAGE INCURRED
1	I	1 FOOT	NO DAMAGE NOTED	4	I	1 FOOT	NO DAMAGE NOTED
2	I	1 FOOT	NO DAMAGE NOTED	5	I	1 FOOT	NO DAMAGE NOTED
3	I	1 FOOT	NO DAMAGE NOTED	6	I	1 FOOT	NO DAMAGE NOTED

TOTAL WEIGHT ON SHOCK TABLE: E-1,1325/10-1, 2407. LBS.

REMARKS

TEST LABORATORY: Lockheed Elec. Co., Inc. Environmental Laboratory

ADDRESS: U. S. Highway 22 Plainfield, New Jersey 07061-1501

SIGNATURE OF TEST WITNESSED: [signature]

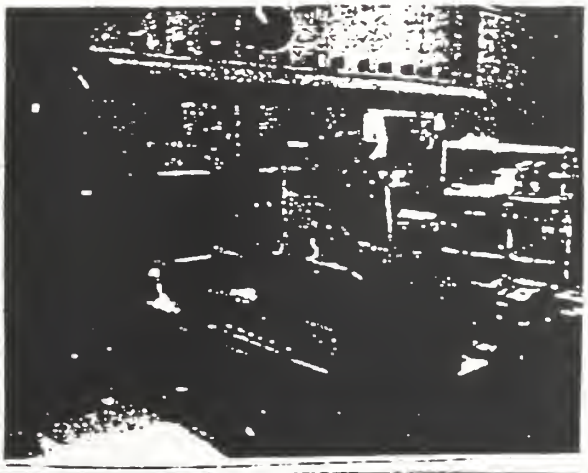

FIGURE 1

SHOCK TEST SETUP, FIGURE 9-1, WITH ANTENNA PARALLEL TO MOUNTING RAILS

FIGURE 2

SHOCK TEST SETUP, BLOW #2, ROTATED 90°, FIGURE 9-1, ANTENNA PERPENDICULAR TO MOUNTING RAILS

FIGURE 3

SHOCK TEST SETUP, BLOW #1, 30° INCLINE, FIGURE 10-1, ANTENNA PERPENDICULAR TO MOUNTING RAILS

FIGURE 4

SHOCK TEST SETUP, FIGURE 10-1, BLOW #2, WITH THE ANTENNA ROTATED 45° FROM BLOW #4

FIGURE 5

SHOCK TEST SETUP, FIGURE 10-1, WITH ANTENNA PARALLEL TO MOUNTING RAILS

A P P E N D I X A

ACCELEROMETER LOCATIONS

X-Y PLOTS

This Appendix contains 44 pages

ACCELEROMETER LOCATION AND

X-Y PLOT INFORMATION

CHANNEL NO.	LOCATION
1	INPUT AT BASE OF UNIT
2	MOUNTING RAIL ABOVE FIXTURE FIG. 9-1
3	ADAPTER BETWEEN ANTENNA AND PEDESTAL
4	CENTER TOP OF ANTENNA
5	TOP OUTER END OF ANTENNA
6	DRIVE MOTOR MOUNTING FLANGE

* * * * * * * * * *

X - Y PLOT INFORMATION

X = TIME IN MILLISECONDS

Y = ACCELERATION "G" PEAK

EU = ENGINEERING UNITS (ACCELERATION "G" PEAK)

FILTERING = .2 - 200 Hz

EXAMPLE = -4.97E1 EU = .49.7 G

ENCLOSURE 4.12-4

ANTENNA PEDESTAL VIBRATION PLOTS

THIS ENCLOSURE CONSISTS OF 23 PAGES

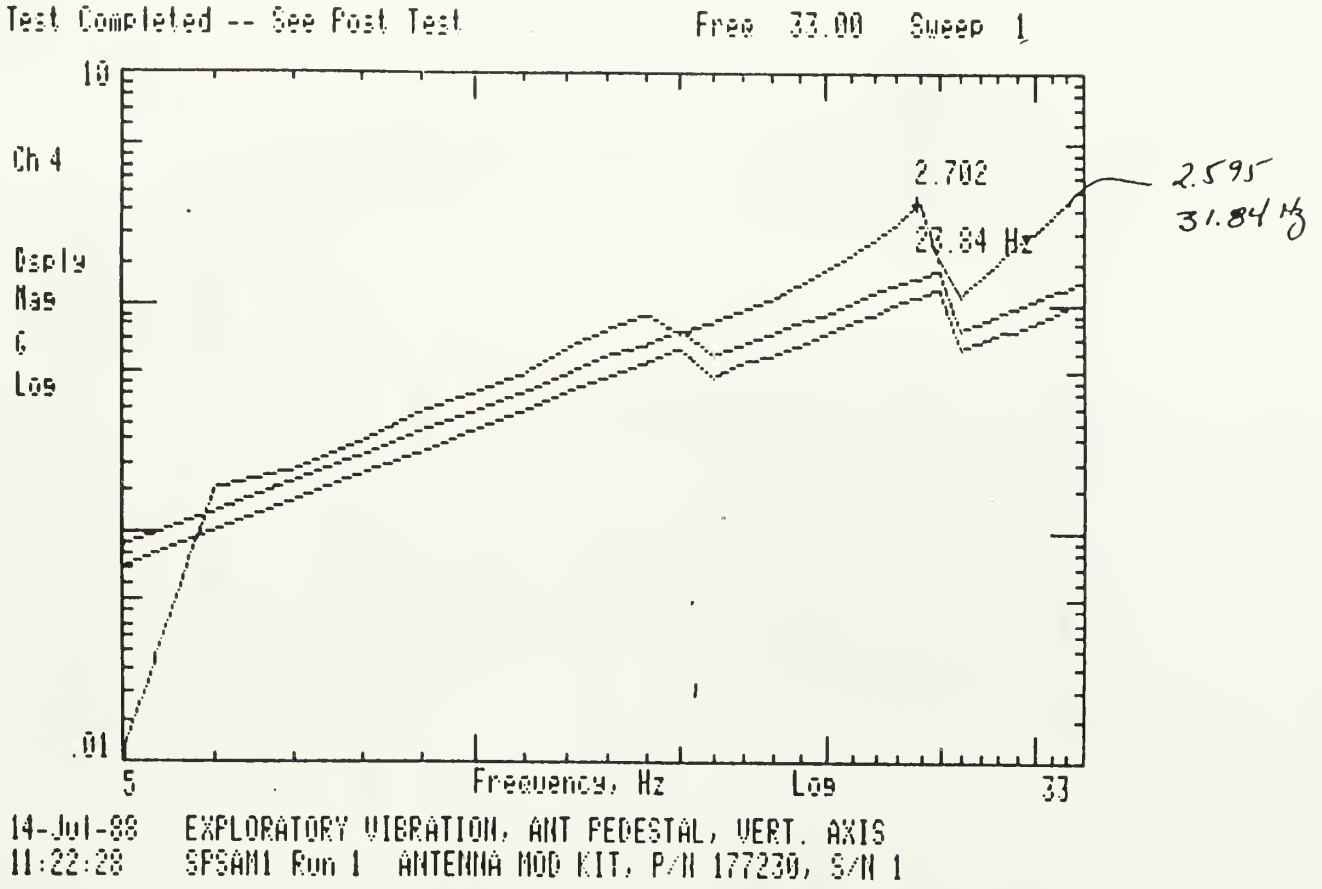

MONITOR ACCELEROMETER
LOCATION: TIP OF ANTENNA

LIST OF REFERENCES

1. Private communication and notes from Norden Systems Inc., Norwalk, Connecticut, 21 March 1994.

2. Mark McLean, Jerry Hill, Richard Cobb and Fred Randall, "Modal Test of JOHN PAUL JONES (DDG–53) Mast and Mast–Mounted Antennas", Naval Engineers Journal, Volume 106, Number 2 (March 1994): 110–117.

3. Lawry, M. H., *I–DEAS Student Guide*, p. 253, Structural Dynamics Research Corp., 1993.

4. Lawry, M. H., *I–DEAS Student Guide*, p. 253, Structural Dynamics Research Corp., 1993.

5. Lawry, M. H., *I–DEAS Student Guide*, p. 254, Structural Dynamics Research Corp., 1993.

6. Lawry, M. H., *I–DEAS Student Guide*, p. 255, Structural Dynamics Research Corp., 1993.

7. Military Specification, MIL–S–901D, "Shock Tests, H.I. (High Impact) Shipboard Machinery, Equipment, and Systems, Requirements for" Prepared by the Naval Ship Engineering Center, 17 March 1989.

8. "Shock Qualification Test Data" provided by Charles Connors, Norden Systems Inc., Norwalk, Connecticut, 21 March 1994.

9. "Shock Qualification Test Data" provided by Charles Connors, Norden Systems Inc., Norwalk, Connecticut, 21 March 1994.

10. "Shock Qualification Test Data" provided by Charles Connors, Norden Systems Inc., Norwalk, Connecticut, 21 March 1994.

11. Messina, G., *MWSM Characterization,* Naval Undersea Warfare Center, New London, Connecticut, June 1993.

INITIAL DISTRIBUTION LIST

		No. of Copies
1.	Defense Technical Information Center Cameron Station Alexandria, Virginia 22304–6145	2
2.	Library, Code 52 Naval Postgraduate School Monterey, California 93943–5002	2
3.	Department Chairman, Code ME/Mz Department of Mechanical Engineering Naval Postgraduate School Monterey, California 93943	1
4.	Naval Engineering Curricular Office, Code 34 Naval Postgraduate Scool Monterey, California 93943	1
5.	Professor Y.S. Shin, Code ME/Sg Department of Mechanical Engineering Naval Postgraduate School Monterey, California 93943	2
6.	Professor J.H. Gordis, Code ME/Go Department of Mechanical Engineering Naval Postgraduate School Monterey, California 93943	1
7.	Mr. Mark McLean Code 03K21 Naval Sea Systems Command 2531 Jefferson Davis Highway Arlington, Virginia 22242–5160	2
8.	Mr. Victor DiRienzo Code 03K21 Naval Sea Systems Command 2531 Jefferson Davis Highway Arlington, Virginia 22242–5160	1

9.	Mr. Joel Bloom Staff Scientist Office of the Secretary of Defense OSD/ODDRE/Life Fire Test Room 3E1060, The Pentagon Washington, D.C. 20301	2
10.	Mr. Jerry Hill NKF Engineering, Inc. 4200 Wilson Blvd., Suite 900 Arlington, Virginia 22203—1800	1
11.	Dr. Thomas Moyer, Jr. NKF Engineering, Inc. 4200 Wilson Blvd., Suite 900 Arlington, Virginia 22203—1800	1
12.	LT Thomas A. Tomaiko U.S. Navy 23 Campus Lane Lake Ronkonkoma, New York 11779	4